HRV analysis of Preterm Infant ECG; Tools, Techniques and Challenges

A thesis submitted towards the partial fulfilment for the degree of
Masters of Engineering
In

Biomedical Engineering

Course Affiliated by Faculty of Engineering & Technology

Jadavpur University

Submitted by

Gouranga Bala

EXAMINATION ROLL NUMBER: M4BMD18002

CLASS ROLL NUMBER: 001630201008

REGISTRATION NO: 137408 of 2016-2017

Under the guidance of
Dr. Monisha Chakraborty
Associate professor,
School of Bioscience and Engineering
Jadavpur University
Kolkata- 700032

School of Bioscience and Engineering

Jadavpur University

Kolkata- 700032

India

2018

Dedicated to the cause of science and truth

ACKNOWLEDGEMENT

I express my heartiest gratitude to my respected thesis advisors Dr. Monisha Chakraborty, Associate Professor, School of Bioscience & Engineering, Jadavpur University for her esteemed guidance, constant encouragement and supportduring the entire period of my project work.

I am grateful to Dr. PiyaliBasak, director, School of Bioscience and Engineering for her constant support throughout the tenure of my master degree program at School of Bioscience and Engineering, Jadavpur University.

Special thanks to Debanjan Parbat, PhD scholar for his invaluable suggestion and friendly guidance and encouragement, which made the laboratory a special place, learnings fun. I express my gratitude and love to all my batch mates without whom the life would be most boring place. They always helped me to keep my spirit high.

I would also like to thank all my seniors, nonteaching stuffs and all my juniors for their kind co-operation.

Last, but not the least, I want to express my profound gratitude and my love for my family who have been the constant support and strength for me to go on with my higher education.

Date: **Gouranga Bala**

DECLARATION

I hereby declare that this submission is my own work and that, to the best of my knowledge and belief, it contains no material previously published or written by another person nor material which has been accepted for the award of any other degree or diploma of the university or other institute of higher learning, except where due acknowledgment has been made in the text. All information in this document has been obtained and presented in accordance with academic rules and ethical conduct.

Place:

……...……..

Date: **GOURANGA BALA**

Registration number: 137408

M.E. (Biomedical Engineering) course affiliated to
Faculty of Engineering and Technology
Jadavpur University
Kolkata, India

CERTIFICATE OF RECOMMENDATION

This is to certify that the thesis entitled "**HRV analysis of Preterm Infant ECG; Tools, Techniques and Challenges**" that is being submitted by Sri Gouranga Bala, in partial fulfillment for the award of degree of Master in Biomedical Engineering of Jadavpur University is a record of bona fide work carried out by him under my guidance and supervision. The project, in our opinion, is worthy for its acceptance.

_____

Dr. Monisha Chakraborty
(Thesis Advisor)
Associate Professor
School of Bioscience and Engineering
Jadavpur University
Kolkata-700032

_____

Dr. Piyali Basak
Director
School of Bioscience and Engineering
Jadavpur University
Kolkata-700032

_____

Dean
Faculty Council of Interdisciplinary Studies, Law and Management
Jadavpur University
Kolkata – 700032

M.E. (Biomedical Engineering) course affiliated to
Faculty of Engineering and Technology
Jadavpur University
Kolkata, India

CERTIFICATE OF APPROVAL**

The forgoing thesis is hereby approved as a creditable study of an engineering subject carried out and presented in a manner satisfactory to warrant its acceptance as a prerequisite to the degree for which it has been submitted. It is understood that by this approval the undersigned do not necessarily endorse or approve any statement made, opinion expressed or conclusion drawn therein but approve the thesis only for the purpose for which it is submitted.

_____ _____

Dr. Monisha Chakraborty
(Thesis Advisor)
Associate Professor
School of Bioscience and Engineering
Jadavpur University
Kolkata-700032

Signature of the Examiner

**Only in case the thesis is approved

Preface

Heart Rate Variability analysis has huge potential to disease detection and prediction. But still we are unable to utilize it due to lack of standard protocol. In these work HRV parameter of preterm infant ECG has been studied. The bio marking capability of HRV parameter has been examined.

Chapter one, describes a brief back ground of electrocardiography, parameters and terminology, ECG acquisition and amplification and the noises related to it etc.

Chapter two is about the literature review of the research work.

Chapter three introduces basic concepts that are required for the project. Such as sampling theorem, discrete Fourier transom, inverse discrete Fourier transform, basics of filtering and wavelet transformation.

Chapter four depicts the methodology of the research work the tool used for the job etc.

In chapter five the results has been presented and discussion about the results is briefed.

In chapter six and seven the conclusion and future prospect of the work has been presented respectively.

CONTENTS

LIST OF ABREVIATION

Abbreviation	Full Form
ECG	Electrocardiography
AV	Atrioventricular
SA	Sinoatrial
BW	Baseline Wonder
PLI	Power Line Interference
MA	Muscle Artifacts
FIR	Finite Impulse Response
IIR	Infinite Impulse Response
WT	Wavelet Transform
PCA	Principle Component Analysis
HRV	Heart Rate Variability
ANS	Autonomic Nervous System
HR	Heart Rate
BP	Blood Pressure
CO	Cardiac Output
RMSSD	Root Mean Square of Successive Differences
SDSD	Standard Deviation of Successive Differences
HF	High Frequency
LF	Low Frequency
VLF	Very Low Frequency
ULF	Ultra Low Frequency
SNR	Signal to Noise Ratio
AR	Auto Regressive
ISI	Inter Symbol Interference
ANN	Artificial Neural Network
SVM	Slope Vector Waveform
LDA	Linear Discriminant Analysis
QSWT	Quadratic Spline Wavelet Transform
FD	Fractal Dimension
VF	Ventricular Fibrillation
VT	Ventricular Tachycardia
DSP	Digital Signal Processing
PSD	Power Spectral Density
ApEn	Approximate Entropy
SD	Standard Deviation
BPF	Band Pass Filter
BSF	Band Stop Filter
TF	Transfer Function

LIST OF FIGURES

Figure No. **Figure Caption** **Page No**

Figure No. **Figure Caption** **Page No.**

[1] INTRODUCTION

Motivation: Cardiovascular disease is one of the leading cause of mortality in recent years. For this reason development of better cardiac diagnostics protocol has gain interest among scientific community. In typical cardiac diagnosis the short term ECG is used and it very few information is extracted from it. But according to physiologists and scientist the information content of the ECG is much more than its current limited use. Heart rate variability (HRV) is the physiological phenomenon of variation in the beat to beat intervals. Its variation contain indicators of current disease in many case. But these indicators may be present at all times or it may occur at randomly at any time. So it is strenuous and time consuming to study and pinpoint abnormalities in ECG data of such long duration. Computer based automated analytical tools are well suited for in-depth study of such long ECG data. With the advent of developed microcomputer technology these diagnosis can be easily done. So Heart Rate Variability analysis has become an important tool in cardiology, these non-invasive measurements are relatively easy to perform, have good reproducibility and also provide prognostic information on patients with cardiac diseases. According to researchers and scientists HRV study is also very useful for understanding the status of the Autonomic Nervous System (ANS). HRV reflects the cardiac system's ability to adapt to the changing external or internal circumstances by detecting and fast responding to the unexpected and unpredictable stimuli. HRV analysis has the ability to assess overall cardiac health and the state of the ANS responsible for regulating cardiac activity.

Electrocardiograph (ECG) is the record of electrical activities of heart over time. To record such electrical activities electrical probes are placed on some predefined regions of our body, where the signal is most legible. This electrodes senses the bio potential variations caused by electrophysiological pattern of polarization and depolarization of cardiac muscle on that region, during each cardiac cycle. In a conventional 12 – lead ECG system 10 electrodes are used, which are placed on the subjects arm, chest and leg. Each ECG lead has its own particular viewing angle of heart [8]. The leads are unipolar, bipolar or augmented in nature, depending on its principle of measurement of the potential difference. Each moment all the 12 leads records the potential variation of heart from 12 different viewing angle. From this recording

the overall direction and magnitude of electrical depolarization of heart can be obtained in a three dimensional space throughout the cardiac cycle.

A healthy heart has an orderly progression of depolarization originating at the pacemaker cells in Sinoatrial (SA) node, spreading out through the atrium, passing through atrioventricular (AV) node down into bundle of His and then into the Purkinje fibers, spreading down and to the left throughout the ventricles. The flow of depolarization has been shown in the figure 1.1. This orderly progression cardiac depolarization gives rise to the characteristic ECG tracing [82] [2]. ECG conveys a large amount of information about the functionality of heart and its conduction system. A clinician can very easily find out the rate and rhythm of heartbeats. Other than these ECG can be used to measure the size and position of the various chambers of heart, presence of any damage to the cardiac muscles or the conduction system, effects of drugs in it, functions of cardiac implants etc.

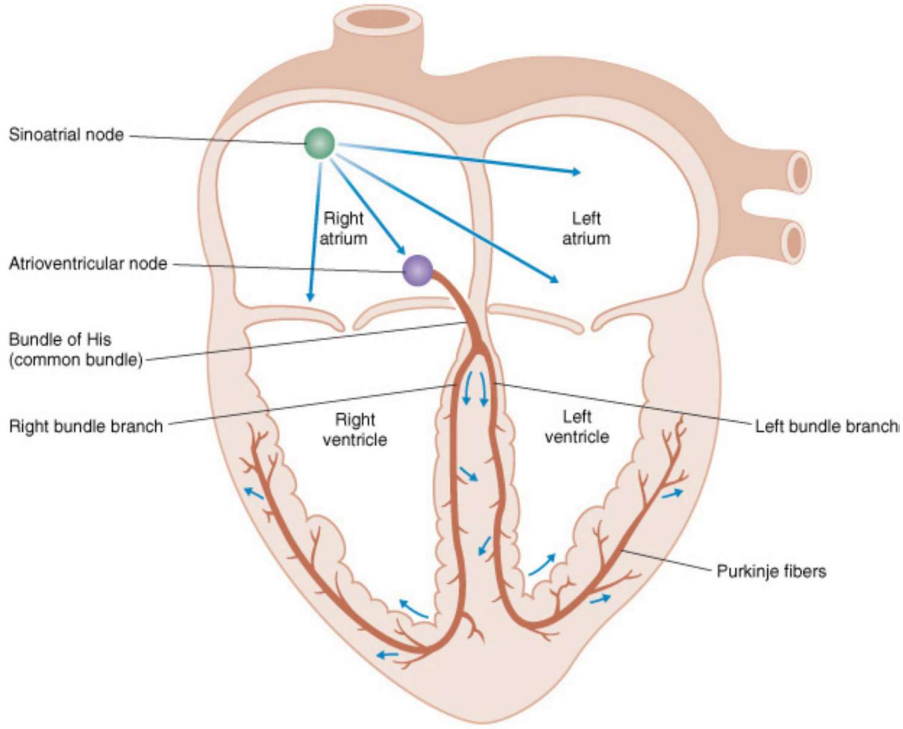

Figure: 1.1. Progression of depolarization wave in heart

A typical ECG wave cycle has some marking point P, Q, R, S and T. These marking is clearly shown in the figure 1.2 and 1.3. Using these point several kind of features further derived, namely peaks or waves, intervals, segments and complex etc. The features are shown in the figure 1.2 and figure 1.3.

One of the most important of these is QRS complex. Which has a very high R peak, two other Q and S inverted peak. Detecting a QRS complex is a very useful step towards others feature extraction of an ECG. The lead II is generally used for QRS complex detection due its best prominence of QRS complex.

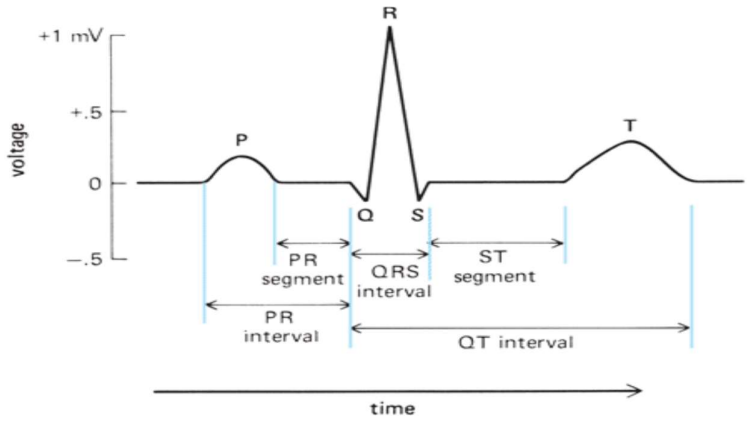

Figure: 1.2 Segments and intervals of an ECG waveform

A brief description of some of the import have been given bellow

P-wave: P wave is the first small peak of the ECG signal, which is caused by the depolarisation of the atrial muscle prior to contraction. The atria contain very little muscle and so the voltage generated during this is quite small.

QRS complex: The QRS complex comes just after the P wave with a comparatively very high R peaks with two inverted small peaks Q and S at each side of it. It is caused by the ventricular depolarisation. Although atrial repolarisation occurs simultaneously, as the amplitude generated by this is very low its effect is not visible.

T-wave: Afterward the QRS complex part again a small peak can be seen in a typical ECG tracing. It is caused by ventricular repolarisation. The time between ventricular contractions, during which ventricular filling occurs, is referred to as the *diastole*.

PR Interval: The time interval between the occurrence of P peak and R peak in an ECG waveform. It should be 0.12s – 0.40s normally.

QT Interval: The time interval between Q point in an ECG waveform and the T point. It should be less the 0.40s normally.

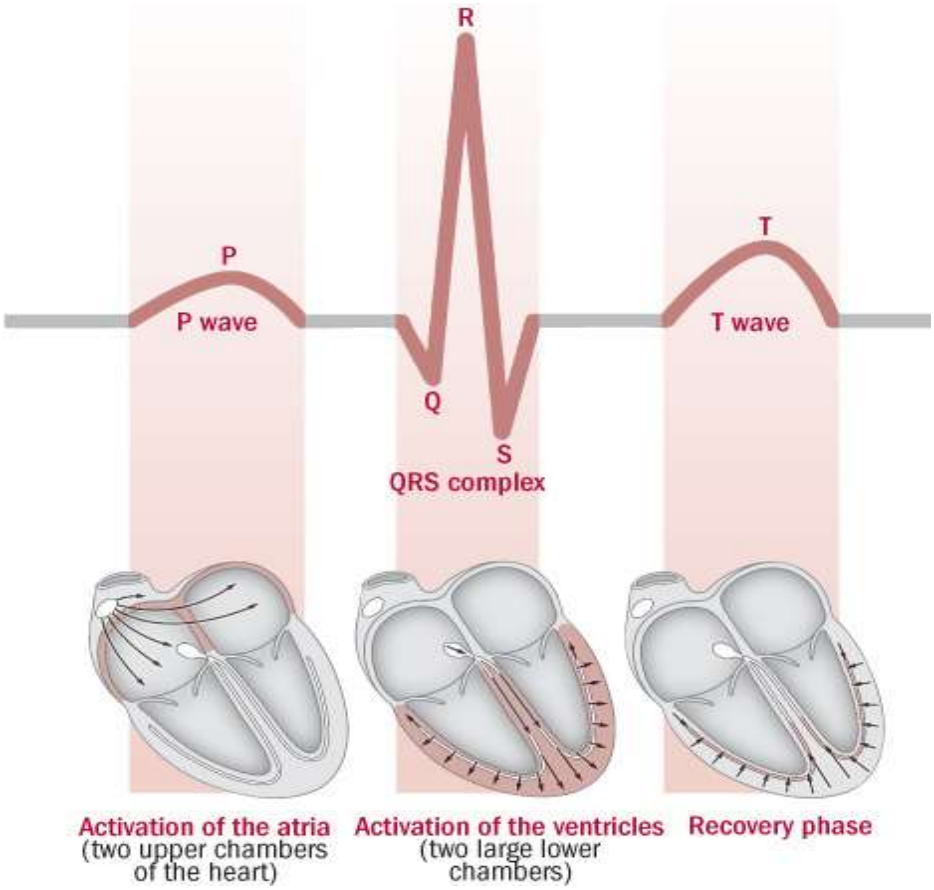

Figure: 1.3 P wave, QRS Complex and T wave and their corresponding depolarization

Although generally the R-peak has the largest amplitude components, the morphology of a healthy ECG tracing can vary greatly from patient to patient with the P- or T-waves dominating or merging at times.

Heart Cycle are to be detected to measure the heart rate variably in it. We define a heart cycle by the segment between two consecutive normal components. For convenience the R wave is taken as the normal component. So in an ECG data stream the R peaks are to be detected to form RR time series. Processing those RR intervals in the RR time series the HRV parameters are obtained.

Heart Rate Variability (HRV) means the variations in inter beat intervals of the heart rhythms or the variations in instantaneous heart rate. This variation has been found to be mainly caused by the sympathetic and parasympathetic nervous system [7] [82]. So HRV has the potential to be a good measure of sympatho vagal balance. Researchers and physiologists for the last few decades has been trying to develop standardized protocol to use it as bio marker of

diseases and other cardio vascular and psychological conditions. It is needed to find the instantaneous heart rate so that the variability in it can be detected.

HRV Parameters can be classified in three categories:

i) Time domain parameters
ii) Frequency domain parameters
iii) Nonlinear parameters

Time domain HRV parameters are relatively simple to derive. The time domain parameters are Mean of NN interval, Standard Deviation of NN interval (SDNN), Variance of NN interval, PNN50, RMSSD, SDSD etc.

Regulation of the Cardiovascular System

Control over the vascular system is required to properly maintain homeostasis by allowing adequate perfusion to reach the tissues and organs throughout the body. The autonomic nervous system is part of the peripheral nervous system that plays an important role in the regulation of cardiovascular system. The autonomic system is divided into two subsystems

i) The sympathetic nervous system
ii) The parasympathetic nervous system.

These two autonomic subdivisions of nervous system behave in such a way so that they are complementary to each other and each functions opposite to the other. They receive feedback from the medullary cardiovascular system to regulate the functions to keep the body stable by fulfilling its requirements.

The general responsibility of the sympathetic nervous system is to utilize the body's resources under stress situation, which has been termed as *the flight-or-fight response.* While the parasympathetic nervous system is responsible for the stimulation of "*rest-and-digest"* or "*feed and breed"* activities [44][42]. That is it regulates the body's activities to keep the body at rest to conserve energy and to control the body functions during rest. Sympathetic nervous system increase the heart rate when required while the parasympathetic nervous system decrease it when the has to return in resting condition. This action is achieved by the modulation of SA rhythm by ANS. The balanced action between the sympathetic and parasympathetic systems generates the rhythmic variation in heart rate activity. An increase in

sympathetic activity will increase heart rate, enhance the blood flow to the skeletal muscles. The increase in heart rate caused by the sympathetic nerves on the SA node is achieved by the rate and force of contraction of the heart. The opposite effect on heart rate and blood pressure is observed when there is an increase in parasympathetic activity. Figure 1.4 showing the ANS regulation of heart rate pathway.

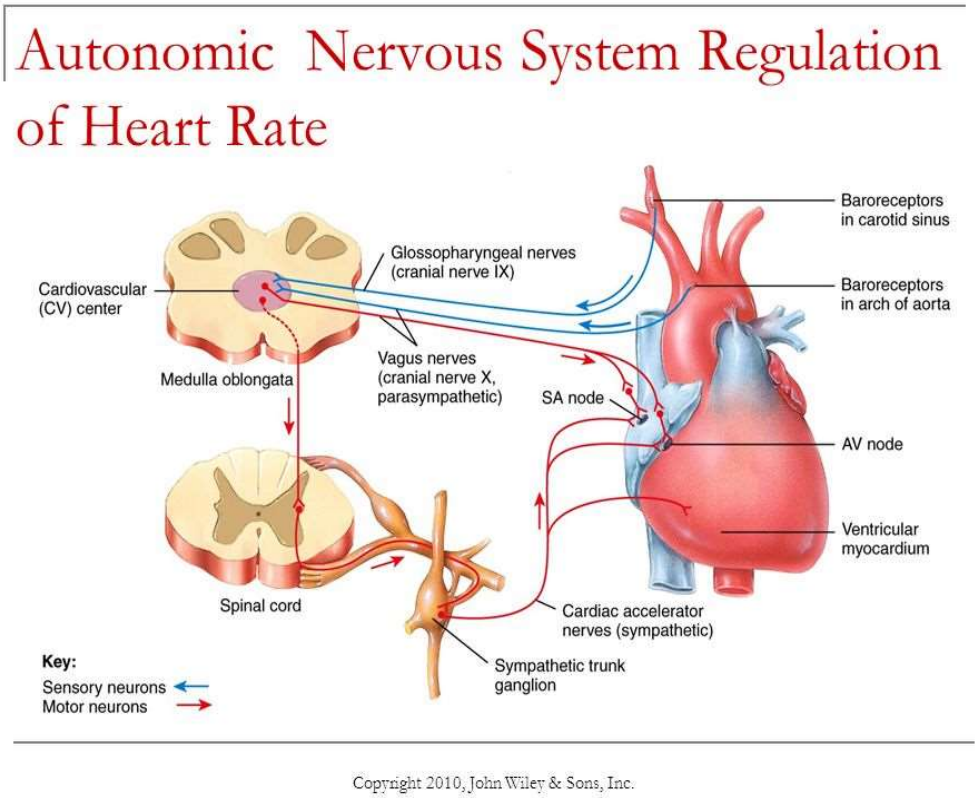

Figure: 1.4. Heart rate regulation by Autonomic Nervous System [43]

In addition to the autonomic system, there are various receptors in the body that also regulate the cardiovascular system. Baroreceptor is one of them. These are mechanoreceptors located in the carotid sinuses and in the aortic arch. Their responsibility is to sense and monitor blood pressure. The stimulation of baroreceptors in the arteries is caused by pressure changes which in effect will cause a response that will increase or decrease heart rate based on the needs of the body. For example, when pressure is low in the arteries, the perturbation will stimulate the carotid sinus. Once the carotid sinus is activated, the baroreceptors will direct signals to the sympathetic system to increase heart rate and vasoconstriction which will cause blood pressure to increase to a normal level. Arterial chemoreceptors are located in the aortic arch and the

carotid sinus and detect the level of carbon dioxide, oxygen, and pH in the blood. An increase in carbon dioxide, decrease in oxygen, and reduction in pH cause an increase in discharge frequency from chemoreceptors. The effect of an increase in discharge frequency from chemoreceptors will cause an increase in vasoconstriction and a slowing of the heart rate. The increase in vasoconstriction will cause an increase in blood pressure, which will stimulate the baroreceptor reflex. Figure 1.5 showing the baroreceptor control flow path.

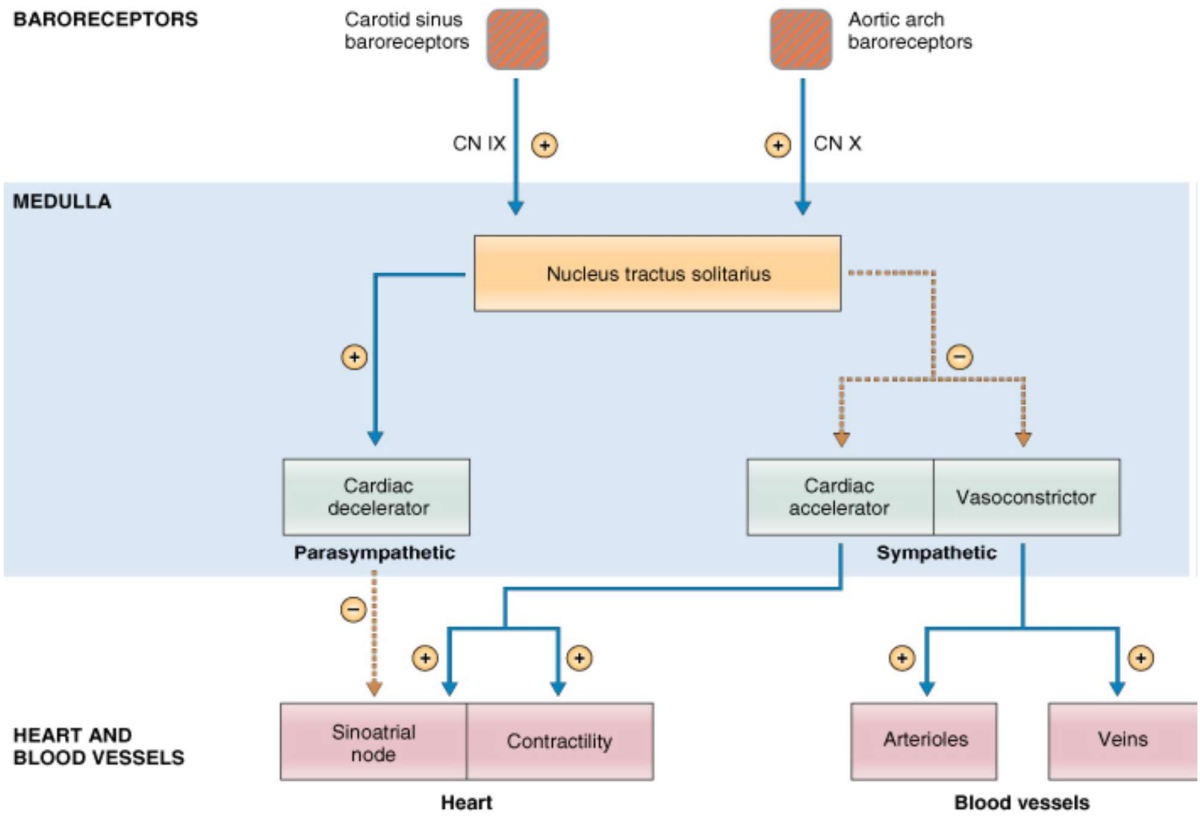

Figure: 1.5. Baroreceptor heart rate regulating operation flow

ECG Signal Acquisition:

An ECG machine amplifies the small bio-potential signal generated by the heart as well as to filter out and internal noise as much as possible. The amplification is mainly implemented through a differential amplifier whereas filtering is completed through common and differential

mode filtering. There is also the Right Leg Drive circuit which cancels noise and maintains the common mode voltage.

ECG signal are very small in magnitude (a few millivolt). Due to this small magnitude, the signals are needed to be amplified in order to study it. Typical bio-potential amplifiers have a very high input impedance so that it is safe from electrocution. This is due to the fact that the signal amplified is being drawn from a living organism so precautions must be taken in order to prevent electric shock. Powerline isolation and protection circuitry are used to limit current through electrodes to safe levels. The output impedance of the amplifier is very low to drive any external load with minimal loss of potential. Again, due to the small size of the signal, the gain should be large. Typically a gain of over 1000 is implemented in bio-potential amplifier circuits. The amplifiers have a high common mode rejection ratio to eliminate large offset signals. Finally, most bio-potential amplifiers are differential. Differential amplifiers only amplify the differential part of the electrode. As noise present effects all electrode same way the noise from the inputs are not amplified thus yielding a higher integrity signal. These amplifiers are called instrumentation amplifier.

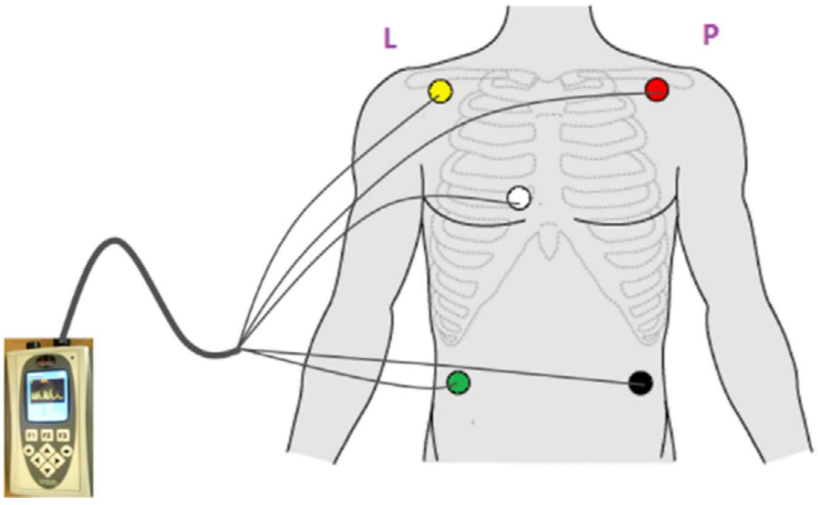

Figure: 1.6. Basic lead placement of ECG device

Differential amplifiers with such characteristics are difficult to find. Thus combinations of differential amplifiers are used to construct what is called an instrumentation amplifier. A basic three-op-amp instrumentation amplifier is shown

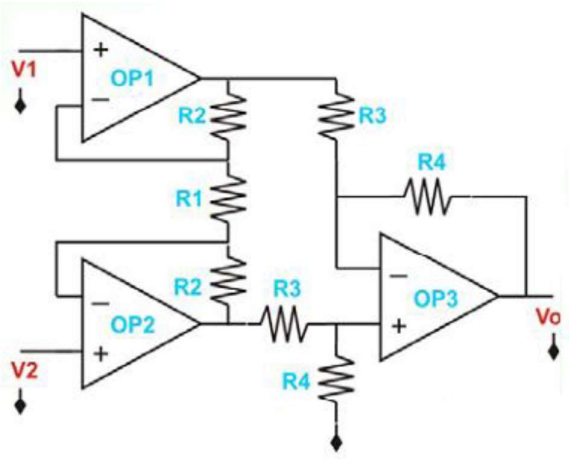

Figure: 1.7. Basic Instrumentation Amplifier Circuit

There are two stages of the instrumentation amplifier to make it fit to the characteristics of an ideal bio potential amplifier. The first stage is the input stage, followed by the gain stage. Figure 1.8 breaks down the two stages.

i) The input stage ideally supplies no common mode gain thus eliminating common mode noise. This part of the instrumentation amplifier works as signal buffer eliminating the need of impedance matching. The three op-amps give the input stage high input impedance and the configuration gives a gain of $G_d = \frac{v_2 - v_4}{v_1 - v_2} = \frac{2R_2 + R_1}{R_1}$. The outputs of the input stage are the inputs of gain stage. The resistance R_1 can act as gain modifier. Changing only the value of R_1 to increase or decrease the gain of the amplifier is a smart circuit design strategy.

ii) The gain stage has low impedance and supplies a differential gain. Overall the amplifier amplifies only the differential component with a gain of $G_d = \frac{2R_2 + R_1}{R_1} * \frac{R_4}{R_2}$ and provides a high common mode rejection ratio. Texas Instruments manufactures an instrumentation amplifier for these purpose for the use in the medical industry. Figure 1.8 shows the block diagram and components of TI make

instrumentation amplifier INA333. This Integrated Chip allows the user flexibility of adjusting the gain as required while keeping the error in minimum.

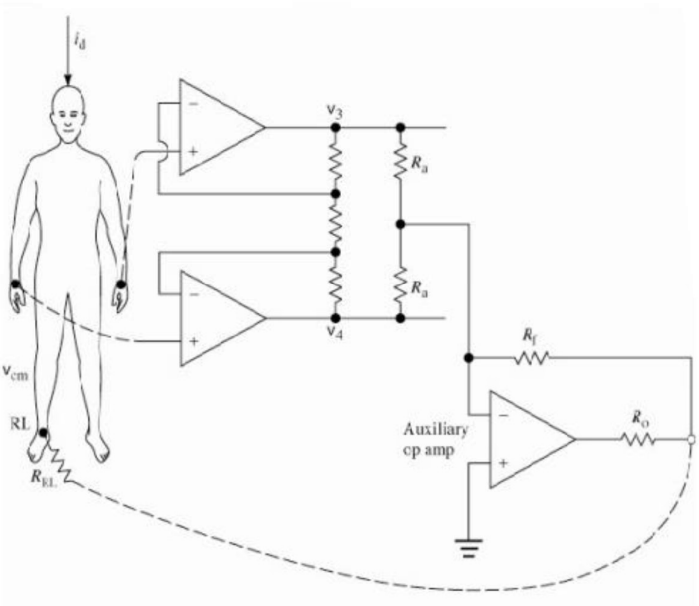

Figure: 1.8. Instrumentation amplifier of ECG with reference to human body

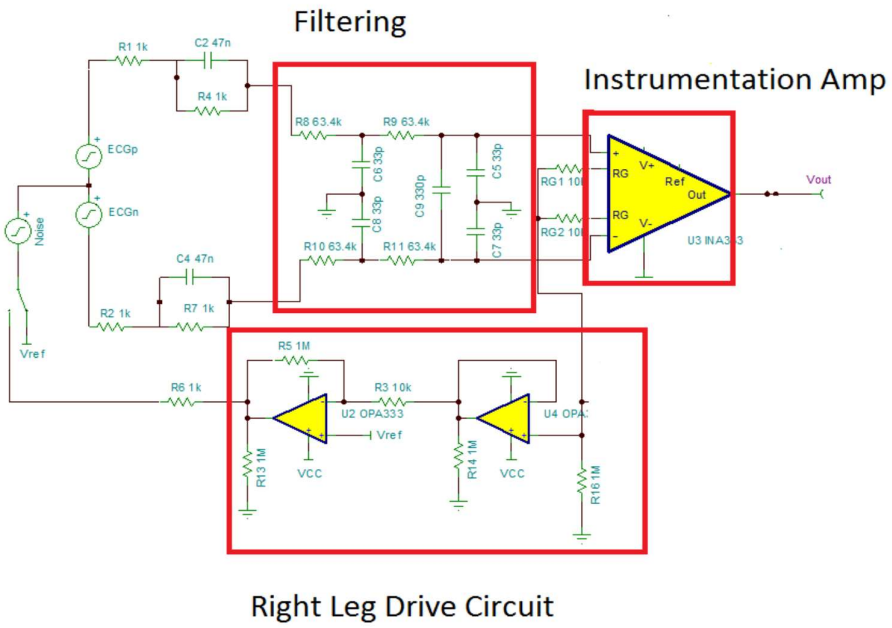

Figure: 1.9. ECG device block diagram.

Noise and Artefacts:

Power-line interference Noise (PLI): Power line interference (PLI) is one of the most common types of noise present in an ECG signal. The connecting wires of the ECG devices acts as antenna. Those Cables are prone to electromagnetic interference (EMI) of frequency (50 Hz or 60 Hz) by the power supply lines. Sometimes the recordings are totally dominated by this type of noise. Removing (filtering) such PLI signal is a significant challenge, as the frequency of the power line signal lies within the frequency range of the ECG signal [7, 8]. PLI is a significant source of noise during bio-potential measurements. EMI degrades the signal quality and disturbs the tiny features that may be crucial for monitoring and diagnosis, and it is observed that it can strongly distort bio potentials. Various biomedical signals contain distinct features in the time-domain analysis. It is seen that the PLI can contaminate the ECG recordings, due to differences in the electrode impedance and stray currents through the patient, cables, or in instruments with a floating input for a higher patient safety. An ECG signal corrupted with PLI is illustrated in Figure 1.10b showing an ECG signal effected with power line interference.

Electromyogram (EMG) Noise: The Electromyogram (EMG) noise is generated by the activity of the muscle. When a muscle contracts or expands there depolarization or repolarization happens. This generates an electrical potential, which is a noise to ECG signal. The EMG consist of a maximum frequency of 10 KHz. Sections of ECG may be interfered and corrupted by surface EMG which causes difficulties in data processing and analysis. Figure 1.10c showing an ECG signal effected by EMG noise.

Baseline Wander: Baseline wander is a low-frequency noise component present in the ECG signal. This is mainly due to respiration, and body movement. Baseline wander disturbance is especially dominant electrocardiography during exercise, and in ambulatory and holter monitoring. The range of frequency in which baseline wander is dominant is typically less than 1.0 Hz, however for exercise ECG this range can be wider. Baseline wander have frequency greater than 1Hz. This low frequency noise, Baseline wander causes problem in detection and analysis of peak. Figure 1.10a showing an ECG signal corrupted with baseline wander.

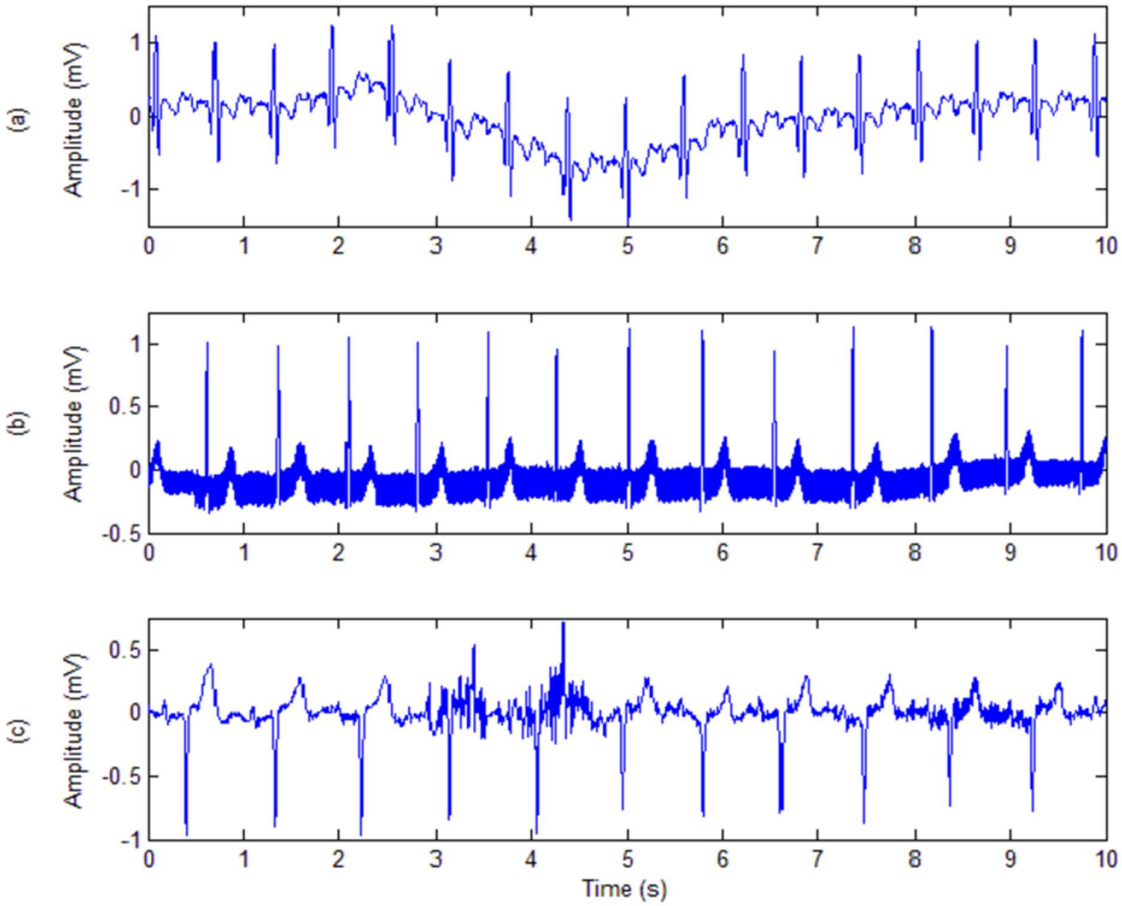

Figure: 1.10 a) ECG signal effected Baseline Wander, b) ECG signal effected by PLI
c) ECG signal effected with EMG noise

Channel Noise: Channel noise introduces when ECG signal is transmitted through channels. This is due to the Poor channel conditions. It is mainly white Gaussian noise which contains all frequency components.

Electrode Contact Noise: Electrode contact noise is caused by the loose contact between the electrode and the skin, or the decreased conductivity due to perspiration or other skin related issue, which effectively disconnects the measurement system from the subject. The noise is of duration 1s.

Motion artefacts: Motion artefacts are transient base line changes caused by changes in the electrode-skin impedance with electrode motion. As this impedance changes, the ECG

amplifier sees a different source impedance which forms a voltage divider with the amplifier input impedance therefore the amplifier input voltage depends upon the source impedance which changes as the electrode position changes.

***

[2] LITERATURE REVIEW

2.1 Signal Acquisition:

ECG is a non-invasive technique to examine the electrical activity of heart [1, 2]. The frequency range of an ECG signal span over 0.67 Hz to 120 Hz, the minimum frequency of 0.67 Hz is observed when the pulse rate is very low nearly 40 beats/min [3]. The Low frequency components of an ECG wave form mainly consist of P and T waves, its band is around 5 Hz to 9 Hz [4, 5], while QRS complex stays at higher frequency range. Digital signal processing (DSP) techniques are applied in signal acquisition in Electrocardiography as it can eliminate the noise very efficiently at a very low cost. But the signal to noise ratio (SNR) effects the performance of such techniques very much while sampling according to Elgendi et al., 2014 [6]. Other than this, ECG contains interferences caused by 50 Hz (60 Hz fir some country) power supply. The power line interference (PLI) lies in the frequency band of the ECG itself, so removing PLI without effecting the original ECG signal is a great challenge [7,8]. High performance instrumentation amplifier along with a right-leg circuit and 50 Hz notch filtering is the standard method in ECG acquisition system to attenuate such noise (Webster, 2010) [9]. Lobodzinski and Laks noted that improvements to measure discernible QRS and P waveforms is required for long term ECG monitoring by ECG devices, in the presence of noise [10]. The Inter signal interference (ISI) of ECG amplitude also has an impact on the quality of sampling too. A low amplitude signal, when converted through analog to digital converters (ADC) with comparatively high frequency range, has a poor quantization, reducing the SNR (Oppenheim and Schafer, 2010) [11]. For ECG acquisition system this is the case. The bio potential have very low amplitude value. But it has a wide frequency range. In order to improve that, the gain of the ECG amplifiers can be manually adjusted for each subject and each lead. Intra-individual variability of ECG amplitude is also observed in long-term ECG acquisition, it is mainly caused by electrolyte drying or movements of electrodes. Many researcher have proposed a method of adjusting the amplifier gain to get clean signal during long term ECG acquisition [12-15].

2.2 Denoising:

The removal or reduction of baseline wanders and power line interference from biomedical signals has been studied since ages and lots of advanced techniques have been proposed for that. Many approaches have been reported in the literature to address ECG enhancement. Some contributions have proposed solutions using a wide range of different techniques, which include maximally decimated filter banks and nonlinear filter banks, advanced averaging, wavelet transform, filtering using adaptive technique, singular value decomposition, and principle component analysis to name a few. In all ECG devices, typically digital FIR filters are used to filter and select the ECG signal in the presence of different interference signals, the filters can be classified as: Low pass filter (LPF) which is implemented to remove the undesired high frequency noise signal. High pass filter (HPF) is implemented to remove the low frequency noise signal. Band stop filter (BSF) is used to remove the noise signal for power line frequencies of 50, 60 Hz. BSF to remove the noise signal for muscles with frequencies of 25, 35, 45 Hz.

Van Alste et al. presented a method of removal of baseline wander and PLI with the implementation of FIR filter with reduced number of taps [16]. Slonim et al. also presented an FIR based filtering in [17], Chavan et al and Coumo et al presented an approach to reduce BW and PLI using IIR filtering approach [18, 19]. Coumo et al did it without the implementation of FFT, which requires special optimization. Resulting in a very simple program.

Alfonso et al presented a filter banks approach [20], which is a sub-band processing, removed noise from the ECG. It is significantly better than mean, median averaging method.

Other than this polynomial filter [21] and Wiener filter [22] have been proposed in the literature to minimize artefacts. Other approaches for ECG denoising include adaptive filters, namely the least mean square (LMS),recursive least square (RLS) and their variants such as the block LMS(BLMS), normalized sign-sign LMS (NLMS) etc., [23-31].

In [32], Mbachu et al presents a method of designing LPF, HPF, BSF with Kaiser window where these three filters are serially connected which process the signal within the range (from 0 to 100 Hz), and with order of 200 for every filter and with interference signals attenuation of 13 dB

In [33], Verma presents a digital Notch filter design using Hamming window to remove the effect of power line interference (PLI) with frequency of 50 Hz, which achieves 13.4dB attenuation. Also, presents an adaptive filter design to remove the effect of PLI and attenuation of 34.2 dB is obtained.

In [34], Madhukar Narsale et al. present a digital Notch filter design with frequency of 50 Hz and with band width of 45 to 55 Hz. They have implemented this filter on FPGA with sampling frequency of 500 Hz, and attenuation of 13 dB

In [35], Sharma and Dalal have presented a FIR filter whose order is 450 and different windows have been applied to remove the effect of power line interference, which has achieved the attenuation of 18 dB.

McManus et al. developed procedures that estimate baseline drift using cubic spline, polynomial, and rational functions. 50 electrocardiograms (ECGs) have been used as a set, each of 2.5-sec duration. Baseline stability was significantly improved by following of any of these procedures except rational function approximation. Amplitude histograms after implementing subtraction of estimated baseline distortions showed only small baseline variations over the recording period. For validation of the estimation procedures, 10 ECGs with artificial baseline drift were constructed and analysed using mean square error calculations [36].

Sornmo et al. has tried applying the time-varying filtering to the problem of baseline correction. The cut-off frequency of a linear filter is efficiently controlled by low-frequency characteristics of the ECG signal. Sampling rate decimation and interpolation has been used so that the design of a filter for baseline reduction can be treated as a narrowband filtering problem. All filters that have been selected and implemented have a linear phase response to reduce distortion. The performance of the method implemented was studied on ECG signals with different types of simulated baseline wander. The results were compared with the performance of time-invariant linear filtering and cubic spline interpolation [37].

A method that can be implemented for removing low frequency interference from an ECG signal is presented by Allen et al. which act as a simple alternative to more computationally intensive techniques. The performance of the method was evaluated by examining changes in body surface iso-potential map feature locations, due to baseline wander. The results show that even though the baseline wander can seriously interfere with iso-potential map features, integrity can be restored by relatively simple methods [38].

Choy TT, Leung P M. have implemented 50 Hz notch filters for the real time application on the ECG signal. That filter was capable of filtering noise (by 40 dB) with bandwidth of 4Hz and causes the attenuation in the QRS complex [39].

Markovsky used Band-pass, Kalman, and adaptive filters for removal of resuscitation artifacts from human ECG signals. A database of separately recorded human ECG was used f or evaluation of this method. The performance criterion considered is the signal to-noise ratio (SNR) improvement, which is defined as the ratio of the SNRs of the filtered signal and the

given ECG signal. The results show that for low SNR of the given signal, a band-pass filter yields the good performance, on the other hand for high SNR, an adaptive filter yields the good performance [40].

Lebedeva SV et al has described and demonstrated the structure and algorithm of a digital suppression filter for circuit noise at 50 Hz. The filter is seen slightly corruptingthe electro-cardio-graphic signal [45].

Daqrouq [46] had used discrete wavelet transform (DWT) for ECG signal processing, specifically for reduction of ECG baseline wandering. Thediscrete wavelet transformhas the properties which enable good representation of nonstationary signal such as ECG signal and divide the signal into different bands offrequency. This enables the detection followed by the reduction of ECG baseline wandering in low frequency subsignals. For testing presented method, ECG signals taken from MIT-BIH arrhythmia database are considered. The method has been evaluated and compared with the traditional methods such FIR and averaging method and with advanced method such as wavelet adaptive filters (WAF).

Zhang [47] approached for BW correction and denoising based on discrete wavelet transformation (DWT). They estimate the BW via coarse approximation in DWT and they recommend how to select wavelets and the maximum depth for decomposition level. They have reduced the high-frequency noise by implementing Empirical Bayes posterior
Median wavelet shrinkage method with level dependent and position dependent thresh holding values.

Sayadi [48] presented a method for ECG baseline correction which implements an adaptive bionic wavelet transform (BWT). By using BWT, the resolution in the time-frequency domain can be adaptively adjusted not only by the signal frequency but also by the signal amplitude which is instantaneous and its first-order differential. Firstly estimation of the baseline wandering frequency is obtained followed by the adaptation which can be used only in three successive scales. The mid-scale has the closest centre frequency to the estimated frequency. Thus the implementation is possibly time consuming.

Methods of decomposing the signals into sub-components for noise reduction have become popular and were proposed for denoising the ECG signals. They include the independent component analysis (ICA), singular value decomposition (SVD), empirical mode decomposition (EMD), and ensemble EMD (EEMD) [49-53]

Soft, hard and adaptive thresholding methods have also been pro-posed on EMD and EEMD schemes [54]. Wavelet transformation (WT) has been shown to be a powerful tool for denoising signals in the frequency domain [55, 56] and has been proposed for ECG denoising

[57-63]. It has conventionally been used by applying soft or hard thresholds on the obtained discrete WT (DWT) coefficients [64, 65]. A combination of DWT with Wiener filtering has been proposed by Kesler et al [66].

In another scheme, the DWT and Neural Networks (NN) are combined to minimize the noise in ECG and have shown to provide better performances than conventional wavelet methods [67-69].

***Detrending of RR Series*:** Sometimes the RR interval time series includes low frequency baseline trend components. Many detrending techniques are available to remove these trend components. The detrending options include removal of the first or second order linear and nonlinear trends. The smoothness priors method presented in [86] can be used to remove these trends. Ruha et al has developed a techniques to derive the timing accuracy of the built-in QRS detection system [87].

2.3 Heart Rate Variability:

Earlier it was believed that the heart beats regularly with a fixed rate. It was after the technological advancement when more precision of measurements of heart rate (HR) were done some amount of variability was observed1. The clinical relevance of heart rate variability (HRV) was first appreciated in 1965 when Hon and Lee [70] observed that fetal distress was preceded by alteration in inter beat intervals before any appreciable changes occur in the actual heart rate. Then Sayers and others had focused attention on the existence of physiological rhythm in beat to beat heart intervals [71-74].

In the late 90's with the recognition of significant relationship between autonomic nervous system and cardiovascular mortality, experimental evidence for an association between lethal arrhythmia and signs of increased sympathetic or reduced vagal activities did encourage the scientific community to develop a quantitative marker of autonomic activity. Recognising this issue *European Society of Cardiology and the North American Society of Pacing and Electrophysiology* jointly formed a Task Force in 1996 to specify and standardise the nomenclature, physiological correlates, and methods of measurements relating to it [1].

The Heart Rate (HR) is defined as the number of heart-beats per minute (per unit time to be precise). The normal HR for any healthy adult ranges from 60 to 100 beats/min at resting

condition [75]. However, HR do not take fixed value. Some variation are presents to respond to the internal and external stress factors. [76-78]. HRV parameters reflects effect of sympathetic and vagal components of the autonomic nervous system (ANS) on the SA rhythm generation. HRV parameters can be categorised in

i) Time-domain parameters,
ii) Frequency-domain parameters, and
iii) Nonlinear indices.

Time domain parameters include-

SDNN: The standard deviation of the normal to normal (NN) intervals.

SDANN: The standard deviation of averages of the NN intervals in all 5 min segments of the entire recording

RMSSD: Root mean square of the successive differences between adjacent NN intervals.

SDNN Index: Mean of standard deviation of all 5 min segment NN interval of the entire ECG

SDSD: standard deviation of differences between adjacent NN intervals.

NN50 count: Number of pairs of adjacent NN intervals differing by more than 50 ms.

PNN50: NN50 count divided by the total number of all NN intervals.

Time domain HRV parameters cannot determine frequency specific power contribution of HRV, due to this limitation, spectral analysis methods are introduced [1].The frequency domain parameters can be of short terms or of long term analysis. The short term frequency domain parameters have a duration around 5 min. The parameters are given bellow-

5 min total power: The variance of NN intervals over the temporal segment

VLF: Power in very low frequency range (<0·04 Hz)

LF: ms2 Power in low frequency range (0·04–0·15) Hz

LF norm: LF power in normalised units, i.e. LF/(Total Power–VLF)

HF: Power in high frequency range (0·15–0·4) Hz

HF norm: HF power in normalised units, i.e. HF/(Total Power–VLF)#100

LF/HF Ratio: LF /HF

The long term frequency domain parameters are-

Total power: Variance of all NN intervals.

ULF: Power in the ultralow frequency range (≤ 0·003 Hz)

VLF: Power in the very low frequency range (0·003–0·04) Hz

LF: Power in the low frequency range (0·04–0·15) Hz

HF: Power in the high frequency range (0·15–0·4) Hz

a: Slope of the linear interpolation of the spectrum in a log-log scale

The long-term frequency domain parameters are calculated over 24 hrs of data

Cardiovascular system consist multiple subsystems that show nonlinear deterministic and stochastic properties [77, 78]. As a result, RR interval time series are often highly nonlinear, random and complex. Due to which time and frequency measures of HRV may not be able to detect subtle, but important changes in the HRV. Therefore, nonlinear methods have been developed to quantify the dynamics of HR fluctuations. Now days, monitoring equipment have expanded their capabilities and specific software tools for HRV analysis are emerging [79-81]. Mostly free software tools offer HRV analysis in time and frequency domain analyses. Some of them include a graphical user interface, and can be used by a wide spectrum of users. Some developers describe their tools without specifying the implementation platform or language. Among the few specific environments for HRV analysis, many tools are proprietary and not made available in the public domain for research purposes. In this paper an attempt has been made to explore the features and limitations of freely online available software tools for HRV analysis in time domain, frequency domain and non-linear domain.

Physiology of HRV: Sympathetic and parasympathetic nervous system generate the control mechanism of Heart Rate Variability (HRV) [1]. Stress, certain cardiac diseases, and many other pathologic states effect the HRV. Berntson et al have given a good review of physiological origins and mechanisms of HRV [82].

Power spectral density (PSD) of the RR series is one of the frequency-domain parameter. Calculation of the PSD estimate may either be done by nonparametric [i.e. Fast Fourier transform (FFT) based] or parametric [i.e. based on autoregressive (AR) models] methods [83]. The power spectral density is analysed by calculating powers and peak frequencies for different frequency bands. Generally the spectrum of HRV is divided into three frequency bands, namely- very low frequency [(VLF) 0 Hz - 0.04 Hz], low frequency [(LF)

0.04Hz - 0.15 Hz], and high frequency [(HF) 0.15Hz-0.4 Hz]. The commonly used frequency-domain parameters are powers of VLF, LF, and HF bands in its absolute and relative values, the normalized power of LF and HF bands, the LF to HF ratio and the peak frequencies of each frequency band (i.e. Mode of VLF, LF and HF band). For the nonparametric or FFT based spectrum power estimates are calculated by integrating the power over the frequency bands whereas for the parametric spectrum is divided into several components and the total band powers are obtained as the summation of powers of these components. A detailed description of this can be found in the work of P. Tikkanen [84].
The parametric spectrum power estimation techniques have been popular in HRV analysis of ECG because of this property.

Complex regulation mechanisms controls the HRV [82]. So it is realistic to presume that HRV also contains nonlinear properties. But the interpretation and understanding of many nonlinear methods are still insufficient. One very simple and easy to comprehend nonlinear method is the Poincar´e plot. It is the graphical representation of correlation between consecutive RR intervals. So the geometry of the Poincar´e plot is essential. A common approach to describe the geometry of Poincar´e plot is to fit an ellipse to the graph [85]. The ellipse is fitted onto the line-of-identity at 45◦ to the normal axis. Then the standard deviation of the points, perpendicular to the line-of-identity is calculated. It is denoted by SD1 which describes the short-term variability of the RR Interval. The short term variability is mainly caused by respiratory sinus arrhythmia (RSA). The standard deviation along the line-of-identity is calculated as SD2 which describes the long-term variability.

HRV and ANS: HRV provides valuable insights into the working of autonomous nervous system (ANS), and can be used for tracking alertness, sleeping state, emotion analysis, arrhythmia detection. It has other applications too, such as estimation of systolic and diastolic blood pressure [95-97]. The control of functions of breathing and blood circulation are related to the autonomic nervous system (ANS). In the literature there are several studies that evaluate the behaviour of the ANS. A common way to measure ANS function is through the power spectral analysis of Heart Rate Variability (HRV). HRV describes the oscillations of intervals between successive heartbeats, reflecting the activity of the autonomic nervous system on the sinoatrial node. Quantitative indices of HRV are obtained from electrocardiogram (ECG) signals. These indices can evaluate changes in autonomic function [82] in physiological aging. The low (0.04 to 0.15 Hz) and high (0.15 to 0.4 Hz) frequency components of the HRV power

spectrum can identify variations in a patient's ANS function [82]. There are, however certain limitations in this technique. Since only the "output" of the system is evaluated, an oscillation in this variable may be due to actual variations in the ANS, but also due to variations in system "inputs", such as respiration. To circumvent this limitation, the Impulse Response (IR) method is also used. The IR characterizes variations of RR intervals independently of respiratory rate. This method was used by Javier [83] using an autoregressive model with exogenous inputs (ARX) and proved to be efficient in coupling healthy individuals

HRV and Hypertension: With the rapid social and economic development, stress induced by varieties of factors in life is affecting ordinary people, and has been considered a key impact factor in health. To prevent stress-related diseases primarily, evaluation of an individual's current stress level is the first step. And studies have shown that stress is caused by an imbalance between external stimulus and individual's ANS controlling ability [91],

Poddar ET. Al conducted a research involving 57 hypertensive patient and 57 normal subject to find the validity of using HRV parameters as a bio marker of hypertension in [88]. The time domain features of HRV for most of the cases have been found to be much lowered for hypertensive patients as compared to normal subjects [8]. Nataranjan ET. El have analysed the HRV of 30 normotensive and 30 hypertensive subjects [89] and concluded that the hypertensive condition could be well monitored and managed with the help of time domain parameters of HRV which are significantly lower compared to normotensive persons. In the work by Urooj ET. El HRV has been calculated for hypertensive patients in Indian population and it has been found that HRV parameters are significantly lowered for hypertensive patients compared to normal subjects [90].

In general, stress levels evaluation involves three processes: Data acquisition, features extraction and classification. According to most articles, data acquisition aims at getting reliable response signals under stress-induced experiment to interpret stress levels. Therefore the design of stress-induced experiment and methods to obtain stress response signals are critical to stress evaluation. Compared to physical, psychological and behavioural signals, physiological signals are more reliable methods to determine stress level.

And these signals are Blood Volume Pulse (BVP), Galvanic Skin Response (GSR) or Skin Temperature. However, they usually require electrodes to be attached to chest or stomach and long period to determine stress level [92]. Feature extraction provides different classification models with features to learn patterns to classify levels of stress. According to most articles

features are extracted through HRV time-frequency analysis, which quantifies the mean or standard deviation of R-R intervals and calculates the power of high and low frequency components of HRV [94].

***

[3] THEORY BEHIND THE WORK

3.1 The sampling theorem

The sampling theorem states that "*A bandlimited signal can be reconstructed exactly if it is sampled at a rate at least twice the maximum frequency component in it.*"

Suppose we have a bandlimited analog signal g(t), whose maximum frequency component is f_m. To recover the signal g(t) exactly from its sampled values of it, it has to be sampled at a rate $f_s \geq 2f_m$. The minimum required sampling rate, $f_s = 2f_m$ is called the *Nyquist rate*.

Let, g(t) be a bandlimited signal whose bandwidth is f_m,

Angular frequency, $\omega_m = 2\pi f_m$.

In the figure: 2.1(a) the time domain representation and in figure: 2.1(b) frequency domain representation counterpart has been shown.

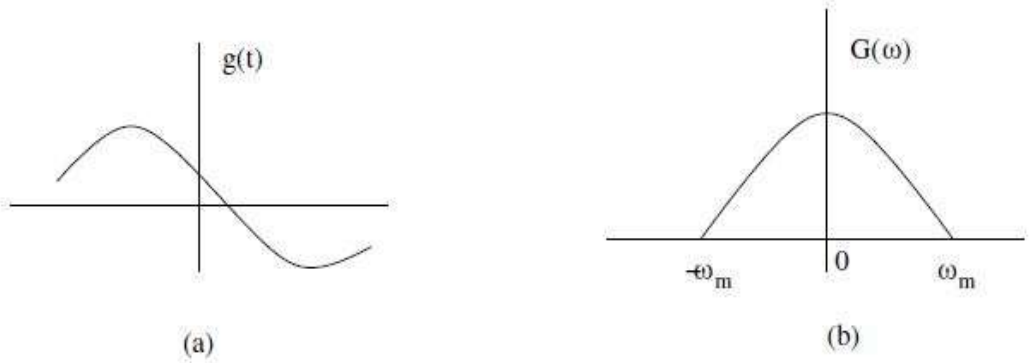

Figure: 2.1 (a) Original signal $g(t)$ (b) Spectrum $G(\omega)$

Assume $\partial(t)$ is the sampling signal with $fs = 1/T > 2fm$.

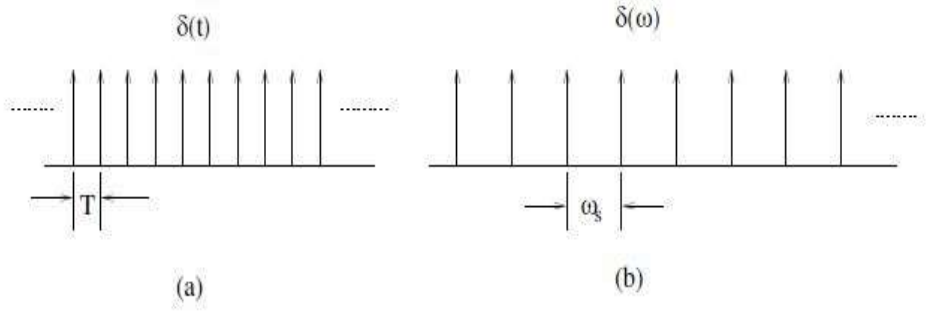

Figure: 2.2 (a) sampling signal $\partial(t)$ (b) Spectrum $\partial_T(\omega)$

Let $g_s(t)$ be the sampled signal. Its Fourier Transform $G_s(\omega)$ is given by

$$F(g_s(t)) = F[g(t)\partial(t)]$$
$$= F[g(t)\sum_{n=-\infty}^{+\infty}\partial(t-nT)]$$
$$= \frac{1}{2\pi}[G(\omega)*\omega\sum_{n=-\infty}^{+\infty}\partial(\omega-n\omega_0)]$$

$$G_s(\omega) = \frac{1}{T}[\sum_{n=-\infty}^{+\infty}G(\omega)*\partial(\omega-n\omega_0)]$$

$$G_s(\omega) = F[g(t) + 2g(t)\cos(\omega_0 t) + 2g(t)\cos(2\omega_0 t) + \ldots]$$

$$G_s(\omega) = \frac{1}{T}[\sum_{n=-\infty}^{+\infty}G(\omega-n\omega_0)$$

If $\omega_s = 2\omega_m$, i.e., $T = 1/2f_m$.
Therefore, $G_s(\omega)$ is given by

$$G_s(\omega) = \frac{1}{T}[\sum_{n=-\infty}^{+\infty}G(\omega-n\omega_m)$$

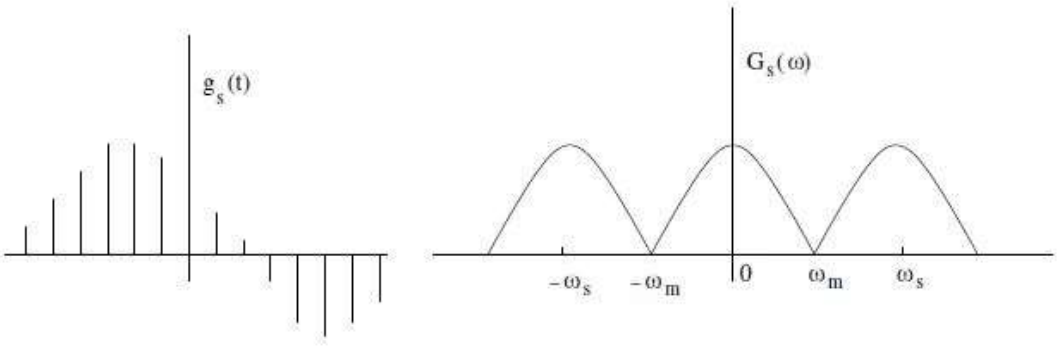

Figure: 2.3 (a) sampled signal $g_s(t)$ (b) Spectrum $G_s(\omega)$

To recover the original signal $G(\omega)$ we need to pass it through a filter with a Gate function, $H_{2\omega_m}(\omega)$ of width $2\omega_m$ and then scale it by T

$$G(\omega) = TG_s(\omega)H_{2\omega_m}(\omega).$$

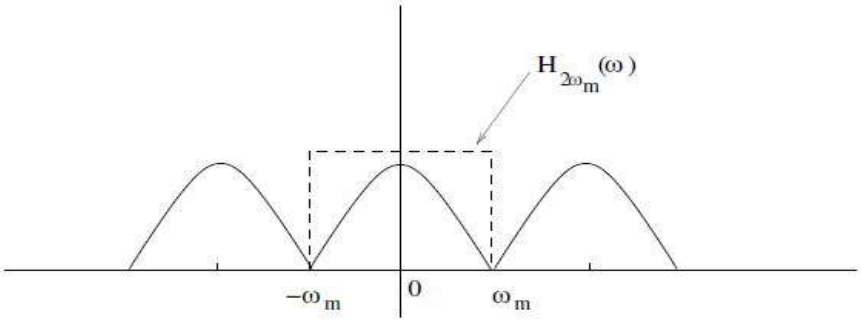

Figure 2.4: Recovery of signal by filtering with a filter of width $2\omega_m$

Aliasing: any frequency greater than $\omega_s/2$ cannot be uniquely presented by sampling it with a frequency of ω_s. The frequency greater than $\omega_s/2$ will interfere with each other and cannot be recovered this phenomenon is called *aliasing effect*.

To avoid aliasing effect we must choose sufficient sampling rate so that our frequency of concern is presentable by the sampled data.

3.2 Discrete Fourier Transform

The Discrete Fourier Transform converts a discrete signal into discrete frequency representation. When we work with digital ECG signal the signals are discrete in nature. The samples are equally spaced over time and functions are sampled at discrete points which are uniformly spaced (i.e. at a time interval of Δt for time series or Δx for spatial data).

The Fourier series of a periodic function can be written in terms of complex exponentials as

$$y(t) = \sum_{k=-\infty}^{\infty} c_k \exp\left(\frac{ik2\pi t}{T}\right) \tag{1}$$

$$\text{Where } c_k = \frac{1}{T}\int_{-T/2}^{T/2} y(t)\exp\left(\frac{-ik2\pi t}{T}\right)dt \tag{2}$$

To construct the discrete Fourier Transform, y(t) has to be replaced by a discrete representation $y_j = 0, 1, 2, \ldots, N\text{-}2, N\text{-}1$ with the sample interval Δt related to the period T by $N\Delta t = T$. Equation (2) becomes a discrete Fourier transform (DFT)

$$c_k = \frac{1}{N\Delta t}\sum_{j=0}^{N-1} y_j \exp\left(-ik\frac{2\pi}{N\Delta t} j\Delta t\right)\Delta t = \frac{1}{N}\sum_{j=0}^{N-1} y_j \exp\left(-i\frac{2\pi}{N} jk\right) \quad (3$$

So the value of c_{k+N}

$$\begin{aligned} c_{k+N} &= \frac{1}{N}\sum_{j=0}^{N-1} y_j \exp\left(-i(k+N)\frac{2\pi}{N} j\right) \\ &= \frac{1}{N}\sum_{j=0}^{N-1} y_j \exp\left(-ik\frac{2\pi}{N} j\right)\exp\left(-iN\frac{2\pi}{N} j\right) \\ &= \frac{1}{N}\sum_{j=0}^{N-1} y_j \exp\left(-i\frac{2\pi}{N} jk\right)\exp\left(-i2\pi j\right) \\ &= \frac{1}{N}\sum_{j=0}^{N-1} y_j \exp\left(-i\frac{2\pi}{N} jk\right) = c_k \end{aligned} \quad (4)$$

$\exp(-i2\pi j) = 1$ for integer j

Thus, c_k is completely defined by specifying N values – it just repeats itself for values outside this range of indices.

In *MATLAB* and in most other implementations of the DFT, the components are specified for

$$c_k, \quad k = 0, 1, ... N-2, N-1 \quad (5)$$

If we specified the Fourier transform based on its derivation from a Fourier series and our understanding that the components at negative and positive frequencies define the phase while summing to yield a real time series, we would specify the components

$$\begin{aligned} c_k, \quad & k = -\left(\frac{N}{2} - 1\right), ... -1, 0, 1, ... N/2 \quad \text{for } N \text{ even} \\ & k = -\frac{(N-1)}{2}, ... -1, 0, 1, ... \frac{(N-1)}{2} \quad \text{for } N \text{ odd} \end{aligned} \quad (6)$$

Since c_k repeats every N values, the ranges defined by equations (4-5) and (4-6) are completely equivalent although the alternate ordering can be confusing at first. To change from one convention to the other we only need to reorder the components on the DFT. In *MATLAB* the function '*fftshift'* does this reordering.

3.3 Inverse Discrete Fourier Transform

The inverse discrete Fourier transform is given by

$$y_j = \sum_{k=0}^{N-1} c_k \exp\left(i \frac{2\pi}{N} jk \right) \tag{7}$$

we can substitute for c_k using equation (3)

$$y_j = \sum_{k=0}^{N-1} \left[\frac{1}{N} \sum_{l=0}^{N-1} y_l \exp\left(-i \frac{2\pi}{N} lk \right) \right] \exp\left(i \frac{2\pi}{N} jk \right) = \frac{1}{N} \sum_{l=0}^{N-1} y_l \sum_{k=0}^{N-1} \exp\left(-i \frac{2\pi}{N} (l-j) k \right) \tag{8}$$

Now the sum over k is a geometric progression of the form

$$S = 1 + r + r^2 \ldots + r^{N-1} \tag{9}$$

With

$$r = \exp\left(-i \frac{2\pi}{N} (l - j) \right) \tag{10}$$

If $l = j$ we can see that the exponent term, r is unity and the sum $S = N$. If $l \neq j$ we can sum the geometric expression by first multiplying equation (9) by r

$$rS = r + r^2 \ldots + r^{N-1} + r^N \tag{11}$$

Subtracting equation (11) from equation (9) yields

$$(1 - r) S = \left(1 - r^N \right) \tag{12}$$

Which gives the following expression for the sum

$$S = \frac{\left(1 - r^N \right)}{(1 - r)} \tag{13}$$

If we substitute equation (10) into (13) the numerator is

$$1 - \exp\left(-i 2\pi (l - j) \right) = 0 \tag{14}$$

So all the $l \neq j$ terms sum to zero and we can see that equation (7) is correct.

❖ ***Fourier Transform Pairs***

If we replace c_k with Y_k in equations (3) and (7) we get a Discrete Fourier transform pair in the conventional notation

$$\begin{aligned} Y_k &= \frac{1}{N}\sum_{j=0}^{N-1} y_j \exp\left(-\frac{i2\pi jk}{N}\right) \\ y_j &= \sum_{k=0}^{N-1} Y_k \exp\left(\frac{i2\pi jk}{N}\right) \end{aligned} \tag{15}$$

Now as for the continuous Fourier Transform, there is an ambiguity in terms of the multiplying term in front of the inverse and discrete Fourier transform. In *MATLAB* the DFT pair is defined by MATLAB

$$\begin{aligned} Y_k &= \sum_{j=0}^{N-1} y_j \exp\left(-\frac{i2\pi jk}{N}\right) \\ y_j &= \frac{1}{N}\sum_{k=0}^{N-1} Y_k \exp\left(\frac{i2\pi jk}{N}\right) \end{aligned} \tag{16}$$

Thus, compared with equation (15) the terms Y_k are N times as big and the inverse DFT requires the introduction of a $1/N$ term. One could also write a symmetric form

$$\begin{aligned} Y_k &= \frac{1}{\sqrt{N}}\sum_{j=0}^{N-1} y_j \exp\left(-\frac{2\pi ikj}{N}\right) \\ y_j &= \frac{1}{\sqrt{N}}\sum_{k=0}^{N-1} Y_k \exp\left(\frac{2\pi ikj}{N}\right) \end{aligned} \tag{17}$$

❖ ***Fast Fourier Transform (FFT):***

From the expression for the discrete Fourier transform shown in equation (16), it is clear that calculating each term for a real time series requires N multiplications of a real number and a complex exponential or $2N$ multiplications. Now all, N terms require $2N^2$ operations which is reduced to N^2 when we remember the symmetry properties of the Fourier transform.

However the Fourier transform can be computed in only $N \log N$ operations when the number of samples is a power of 2 (i.e., $N = 2^M$ where M is an integer). We will not cover the

details, but we can explain it briefly as follows. The forward transform of equation (16) can be written as two series over the odd and even terms to yield

$$\begin{aligned} Y_k &= \sum_{j=0}^{N-1} y_j \exp\left(-\frac{2\pi ikj}{N}\right) \\ &= \sum_{j=0}^{N/2-1} y_{2j} \exp\left(-\frac{2\pi ik2j}{N}\right) + \sum_{j=0}^{N/2-1} y_{2j+1} \exp\left(-\frac{2\pi ik(2j+1)}{N}\right) \\ &= \sum_{j=0}^{N/2-1} y_{2j} \exp\left(-\frac{2\pi ikj}{N/2}\right) + \exp\left(-\frac{2\pi ik}{N}\right) \sum_{j=0}^{N/2-1} y_{2j+1} \exp\left(-\frac{2\pi ikj}{N/2}\right) \\ &= P_k + \exp\left(-\frac{2\pi ik}{N}\right) Q_k \end{aligned} \tag{18}$$

We have expressed Y_k in terms of a sum of two Fourier transforms P_k and Q_k, each for a time series of $N/2$ samples. The reason why this reduces the number of calculations is that because the periodicity of the Fourier transform we can write

$$P_k = P_{k+\frac{N}{2}} \tag{19}$$

So, the calculation of all the terms in P and Q requires only half the number of calculations required for all the terms in G. Now if N is a power of 2 we can keep on subdividing the Fourier series until we are left with series of two-point sequences. The book keeping becomes fairly complex to express, but the net result is that the number of operations is reduced to $N \log N$, an enormous computational saving for long time series. Without the FFT, Fourier transforms would be much less prevalent in computational data analysis.

3.4 Filters:

We know in the ECG signal many noise component is present. It is needed to remove those part of the overall signal. This is called filtering. A filter is a system that remove or allow a certain part signal. Typically filters refers frequency filters, i.e. it removes or allow the part of a signal with a certain frequency range while the signal is passed through it. In this case the filter might be needed to remove the powerline interference present in the ECG signal present or it might be needed to remove the high frequency jittering from an ECG signal. Now depending on the allowing or removal of frequency band filters can be classified as –

a) Highpass filter(HPF)

b) Lowpass filter (LPF)

c) Bandpass filter(BPF)

d) Bandstop filter (BSF)

In the figure 2.5 bellow all the four types of filters has been shown with their transfer function representation. But these filter transfer function are of ideal case. Ideal filters have infinite impulse response and noncausal in nature. The practical Filter cannot produce fully flat response at their passband. Similarly at the stop band they cannot produce perfect zero immediately after crossing the cut off frequency. They have certain amount of ripple present at their pass band as well as at their stop band.

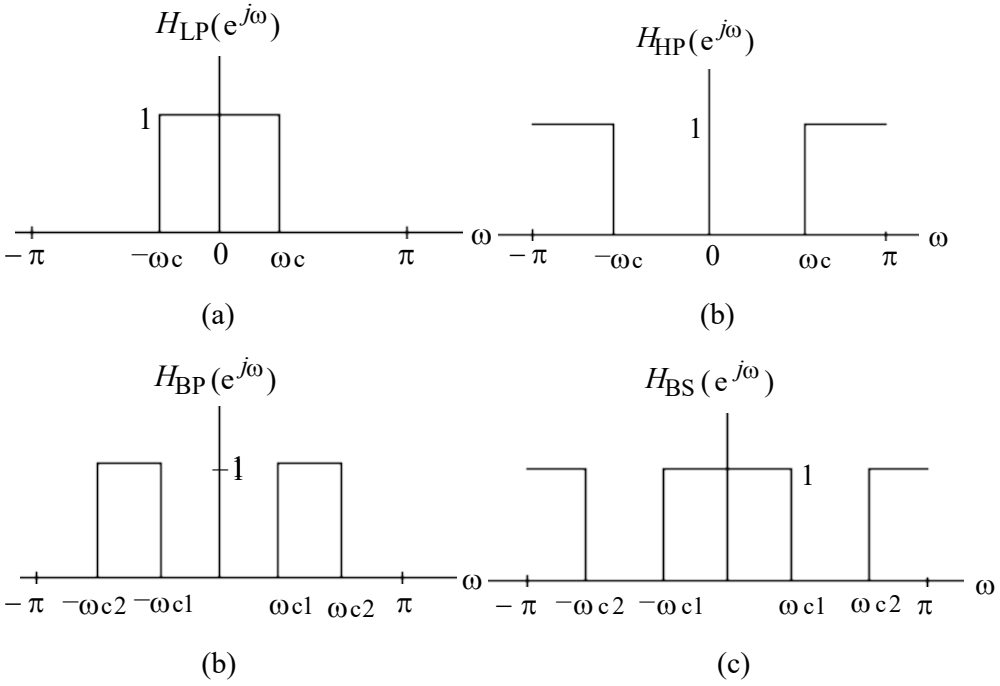

Figure: 2.5. a) Low Pass Filter transfer function; b) High Pass Filter transfer function
c) Band Pass Filter transfer function; d) Band Stop Filter transfer function

Practical filters have some important parameters that we should keep in mind,

ω_p - passband edge frequency

ω_s - stopband edge frequency

∂_p - peak ripple value in the passband

∂_s - peak ripple value in the stopband

These parameters have been shown in the figure 2.6 bellow.

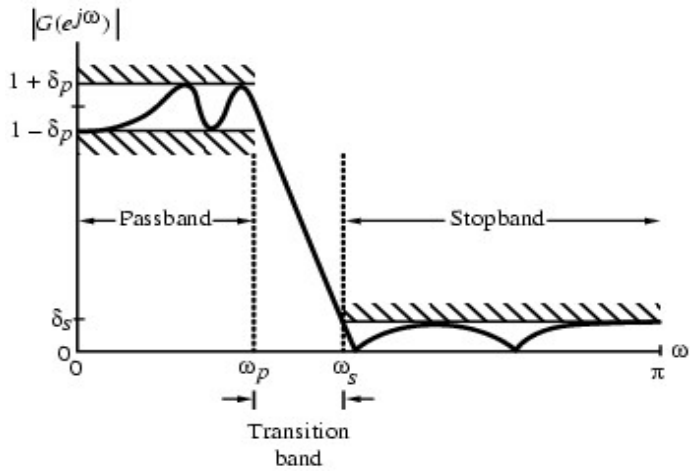

Figure: 2.6. Practical filter specification

The ripple parameters can be represented in dB as

$$G(\omega) = -20\log_{10}\left|G(e^{j\omega})\right|$$

$$\alpha_p = -20\log_{10}(1-\delta_p)$$

$$\alpha_s = -20\log_{10}(\delta_s)$$

We deal with linear time invariant system. So our focus will be on LTI filters and since we are interested in digital signal processing, our concern will be limited to digital filtering.

Linear time invariant (LTI) filters: A class of linear filters whose behaviour does not change over time and whose response is linear over the input range. Linearity implies that the filter meets the scaling and superposition properties

i.e. $x[n] \mapsto y[n] \Longrightarrow \alpha x_1[n] + \beta x_2[n] \mapsto \alpha y_1[n] + \beta y_2[n]$

Types of LTI filters:

Filter can be classified in to two category depending on its impulse response

I. Finite Impulse Response (FIR) filter

II. Infinite Impulse Response (IIR) filter

FIR and IIR filter block diagram has been given bellow in the figure 2.7

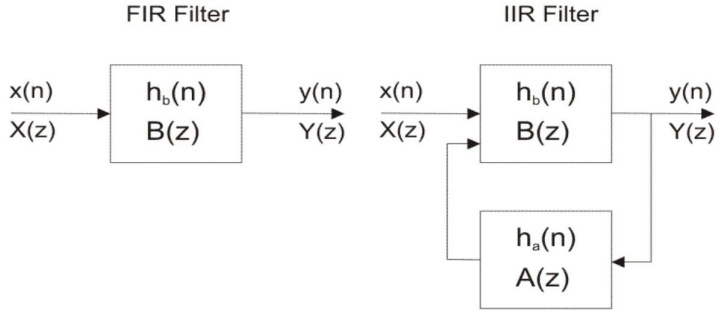

Figure: 2.7. Block diagram representation of FIR and IIR filters

❖ **Finite impulse response (FIR) filter:**

FIR filter can be designed with exact linear phase the filter structure always stable with quantized coefficients. But order of an FIR filter is considerably higher than that of an equivalent IIR filter meeting the same specifications; this leads to higher computational complexity for FIR filtering. Three commonly used approaches to FIR filter design -

(1) Windowed Fourier series approach

(2) Frequency sampling approach

(3) Computer-based optimization methods

The input out relation of a FIR filter given by the difference equation

$$Y[n] = \sum_{k=0}^{M} b_k x\,[n-k]$$

The transfer function of FIR filter is given by

$$H(z) = \sum_{n=0}^{N-1} h(n).z^{-n}$$

❖ **Infinite impulse response (IIR) Filter**

IIR filter is can achieve a particular filtering requirement with fewer parameters. Although it has disadvantage of nonlinearity and instability. IIR filter operate on the current value of input as well on previous values of the output. The difference equation of IIR filter is given by

$$y(n) + a_1 y(n-1) + \ldots + a_N y(n-N) = b_0 x(n) + \ldots + b_N x(n-N)$$

Where $a_{i,,\ldots.}$ b_i are coefficients of the filter

Some very useful IIR filter has been given bellow in brief

- ***Butterworth filter:*** It provides the best Taylor series approximation to the ideal low pass filter response at analog frequencies Ω= 0 and Ω= ∞; for any order n, the magnitude squared response has 2n-1 zero derivatives (i.e., it is maximally flat) at these locations. Response is monotonic overall, decreasing smoothly from Ω = 0 to Ω = 1.
- ***Chebyshev Type I Filter:*** Minimizes the absolute difference between the ideal and the actual frequency response over the entire passband by using an equal ripple in the passband. Stopband response is maximally flat. The transition from passband to stopband is more rapid than for the Butterworth filter.
- ***Chebyshev Type II filter:*** Minimizes the absolute difference between the ideal and the actual frequency response over the entire stopband by using an equal ripple in the stopband. Passband response is maximally flat. The stopband does not approach zero as quickly as the type I filter (and does not approach zero at all for even-valued filter order n). The absence of ripple in the passband, however, is often an important advantage.
- ***Elliptic filter:*** Equiripple in both the passband and stopband. Generally meets filter requirements with the lowest order of any supported filter type. Given a filter order n, passband ripple, and stopband ripple, elliptic filters minimize transition width.
- ***Bessel filter:*** Analog low pass filters have maximally at group delay at zero frequency and retain nearly constant group delay across the entire passband. Filtered signals therefore maintain their waveform in the passband. Digital Bessel filters, however, do not have this maximally at property, and are not supported by MATLAB. Generally require a higher filter order than other filters for satisfactory stopband attenuation.

Some magnitude response of some useful IIR filter has been shown below in the figure 2.8

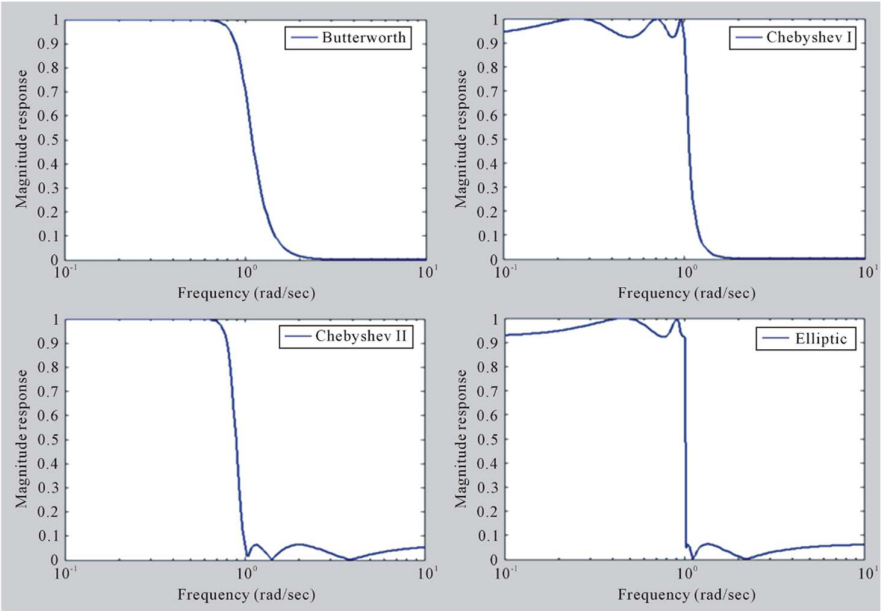

Figure: 2.8. some IIR filter magnitude response

3.5 Wavelet Transform:

The wavelet transform is a decomposition technique where the signal is converted to a summation of a series of wavelets. The series contains scaled version of a mother wavelet. Wavelet transformation provides a way of to analyze a signal simultaneously time and frequency domain. This allows us to denoise an ECG signal more efficiently and better.

Now to compare with Fourier transformation techniques, the Fourier transformation tell the frequency contents of a signal but it cannot say at which time those frequency has been occurring. If a signal is stationary (i.e. each and every frequency component is present in all time) then it has no problem. But in practical signal the frequency might not be present in all time instants. So we can say in frequency spectrum there is zero time resolution. Similarly time domain representation cannot specify the frequency content of a signal at a particular time instant for nonstationary signal. So in time domain there is zero frequency resolution. For this a signal do not have one to one correspondence in time domain to frequency domain. To overcome this problem short time fourier transform (STFT) was introduced. In STFT the signal is seen through a time window in frequency domain. But again if the window employed time window is short then the frequency resolution get limited by it and when the window is wide the time resolution decreases drastically. This problem can be seen in the figures 2.9 and 2.10 bellow.

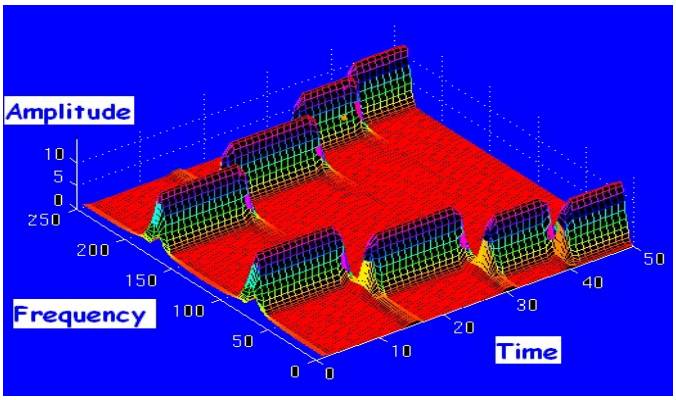

Figure: 2.9. Narrow window STFT

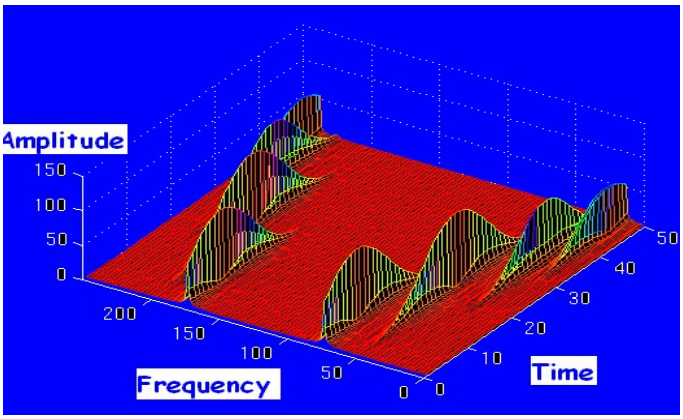

Figure: 2.10. Wide window STFT

Wavelet transform addresses these issues with the help of multiscale analysis.

The continuous wavelet transform of a signal *x (t)* is defined as

$$CWT\ (a,\ b) = \int_{-\infty}^{\infty} x(t)\ \frac{1}{\sqrt{|a|}}\varphi\left(\frac{b-t}{a}\right)dt$$

Where, φ mother wavelet function

a scaling parameter

b shifting parameter

At every possible scale wavelet coefficients calculation is computationally very complex task. The wavelet analysis will be much more efficient if the positions and scales are chosen based dyadic positions and scales i.e. based on powers of two.

Discrete Wavelet Transformation: a discrete wavelet transform is any wavelet transform for which the wavelets are discretely sampled. As with other wavelet transform, a key advantage it has over Fourier transform is temporal resolution. It capture both frequency and location information.

Some commonly used wavelet has been given in the figure 2.11

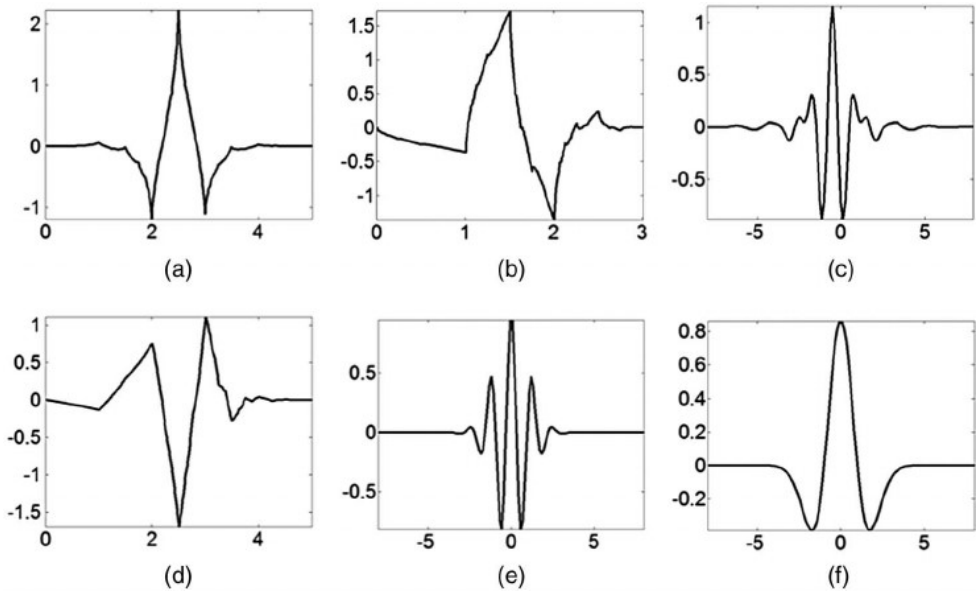

Figure: 2.11. (a) Coif1 wavelet; (b) db2 wavelet; (c) Meyer wavelet; (d) Sym3 wavelet; (e) Morlet wavelet; (f) Mexican hat wavelet

Depending on the signal and the feature to be extracted suitable wavelet is selected. For this thesis work the “haar” wavelet has been used.

***

[4] TOOLS AND TECHNIQUES

Our goal is to find the HRV parameter. For that we need find the instantaneous heart rate or the RR interval of the ECG data. The to find the heart rate general approach is to detect the R peaks of the ECG signal and then considering the gap between two consecutive R peaks is one full cardiac cycle, inverse of the time duration of a cardiac cycle is the instantaneous heart rate.

Detecting the R peaks of a long term ECG signal is not an easy task, especially when the tolerance of error is very low. ECG is an electric potential, essentially it gets effected by any electric field near it, such as the power supply of the ECG acquiring device, electric potentials those are generated by other body parts such as muscle during any movements, breathing, interferences from other electronic equipment, nonlinearity of the device etc.

Presence of these trends and noises in ECG signal makes it difficult to detect the R peak of the accurately. This task of detection of the R peak and the analysis of the derived RR interval has been presented in the flow chart given bellow in the figure 4.1.

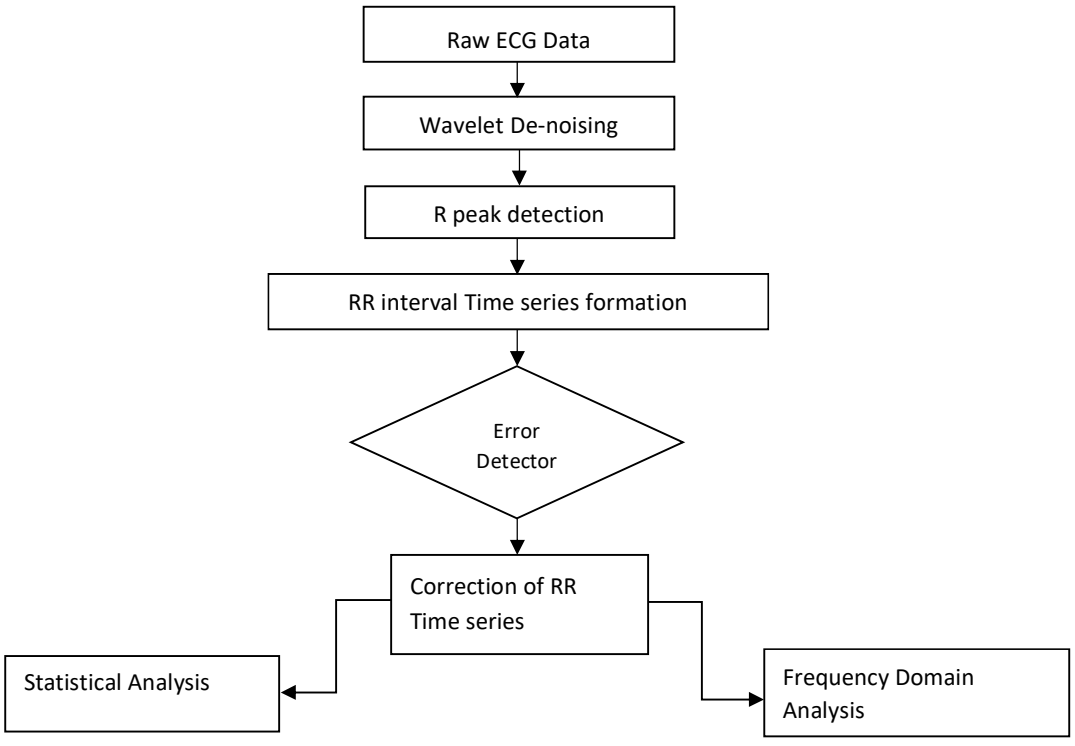

Figure: 4.1. Flow chart of HRV parameter analysis

- **Wavelet Denoising**

The Wavelet transformation is a technique which is used to localize time frequency attributes of a signal. Compared to Fourier Transform, which have a resolution trade-off between time and frequency. Wavelets offer high temporal resolution for high frequency components and high frequency resolution for low frequency components. The wavelet decomposition has been done to emphasize the R peaks of the ECG signal and deemphasize any other peaks present. 8 level Haar wavelet decomposition has been used to highlight the feature of interest i.e. R peak. The threshold to denoise the signal has been selected manually by visually inspecting the threshold where the R peaks are emphasized maximally. Figure 2 showing a signal full of baseline wonder and the after wavelet denoising the baseline wonder has been removed, this is shown in figure 3.

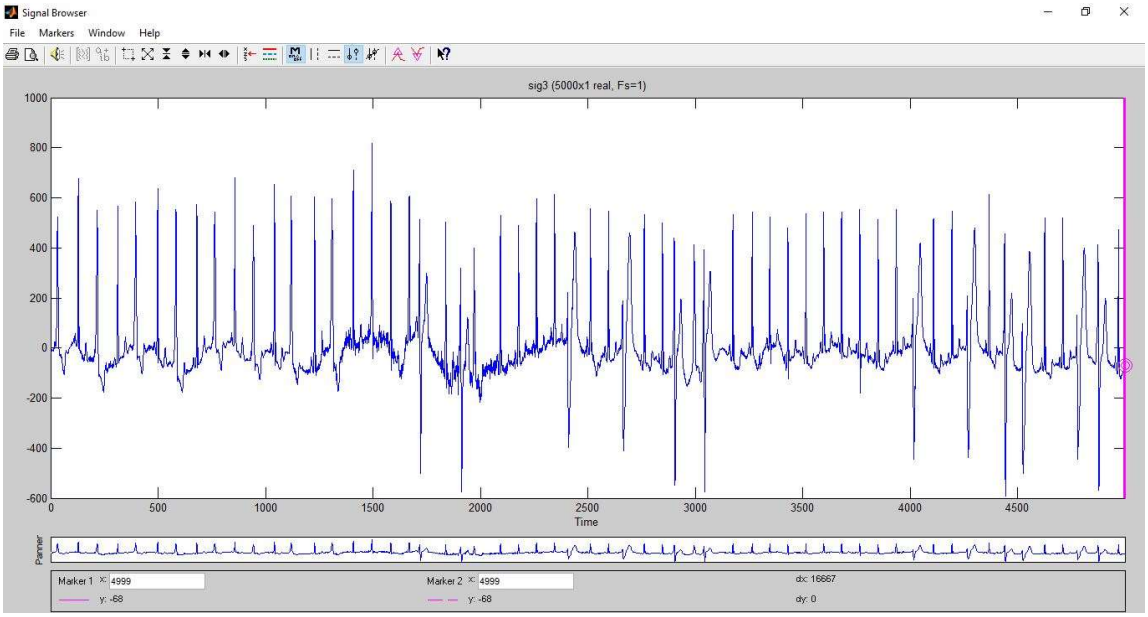

Figure: 4.2. ECG signal with baseline wonder

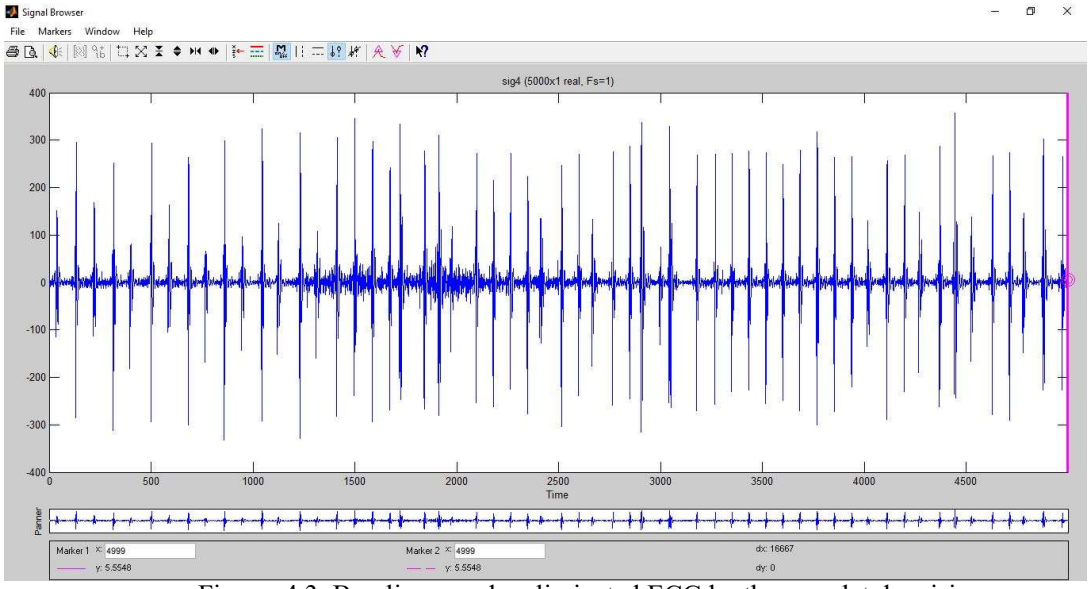

Figure: 4.3. Baseline wonder eliminated ECG by the wavelet denoising

After the denoising is done using wavelet. A peak detection algorithm with as peak distance and peak prominence as threshold has been used to detect the R peaks and to form RR time series.

- **STATISTICAL ANALYSIS**

To compute the statistical parameter the mean, variance and standard deviation from that RR time series has been calculated using the following formula

$$Mean, \mu = 1/N \sum_{i=1}^{N} RR(i)$$

$$Variance = 1/N \sum_{i=1}^{N} (RR(i) - \mu)^2$$

$$SDNN = \sqrt{1/N \sum_{i=1}^{N} (RR(i) - \mu)^2}$$

- **FREQUENCY DOMAIN ANALYSIS**

Frequency domain analysis techniques gives a closer insight into drawing conclusions on the functional abilities of the cardiovascular system. Since the movement of heart is rhythmic, quite often frequency domain analysis techniques is sought for comparative studies.

Different kinds of signals are of different frequency band, so frequency analysis of the RR time series provides important insight. The 0.04HZ to 0.15Hz is called LF band and 0.15Hz to 0.4Hz is called the HF band. The parameter LF/HF i.e. the ratio of power in LF band and the power at HF band denotes the sympathovagal balance of autonomic nervous system.Two digital bandpass filters having passband of 0.04Hz to 0.15Hz and 0.15Hz to 0.4Hz respectively for LF band and HF band have been implemented in MATLAB.

TOOLS:

Through Throughout the Experiment the software package MATLAB® has been used. It is an essential tool for signal processing. A brief description of MATLAB® has been given bellow

- **MATLAB®**

The MATLAB® (*matrix laboratory*) is a multi-paradigm numerical computing environment. It is a proprietary programming language, which has been developed by MathWorks. MATLAB allows users to manipulate, plotting of functions and data, algorithms implementation, user interfaces (UI) creation. Programs written in other languages, such as C, C++, C#, Java, Fortran and Python can be interfaced using MATLAB. Although it is developed primarily for numerical computing, an optional toolbox with MuPAD symbolic engine is there. Which allows the user to access the symbolic computing abilities. For dynamic and embedded systems there is an additional package, Simulink. It adds graphical multi-domain simulation and model-based design features.

MATLAB® is a very useful tool for digital signal processing. Several function specific toolbox is available. Many toolbox functions support C/C++ code generation for desktop prototyping and embedded system deployment. Among them in this thesis SP Toolbox, FD Toolbox and WV Toolbox have been used. A brief has been given bellow.

A. Signal Processing Toolbox

Signal Processing Toolbox software is a collection of tools based on the MATLAB® environment. The toolbox supports a wide range of signal processing operations, from waveform generation to filter design and implementation, parametric modelling, and spectral analysis. The toolbox provides two categories of tools, command-line functions/objects and graphical user interfaces (GUI). The GUI can be accessed by typing a command *'sptool'* in the command line of MATLAB.

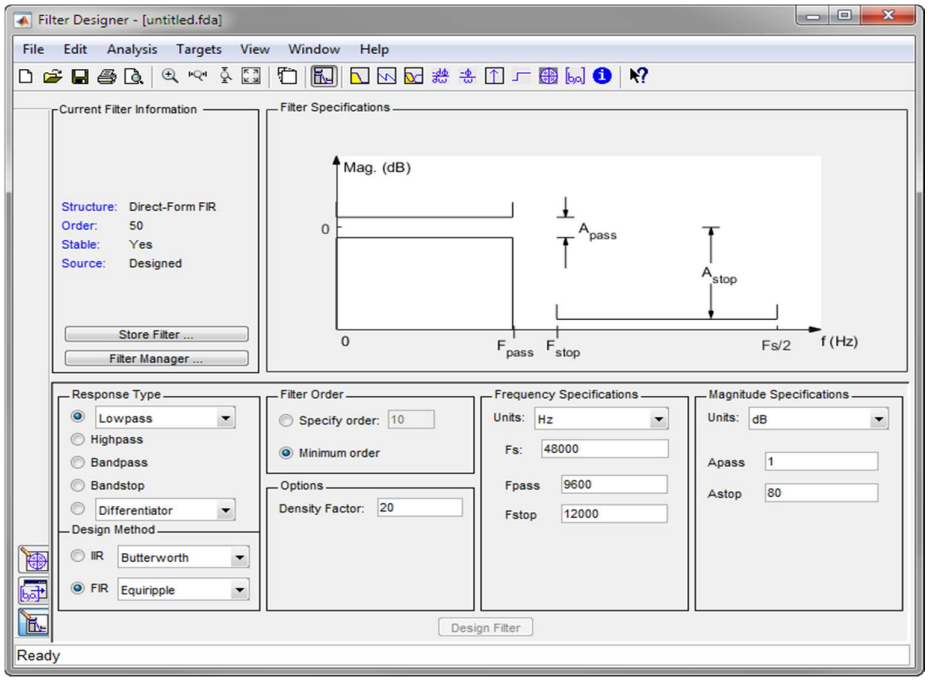

Figure: 4.4. Filter design in SP Toolbox

Command-Line Functions and Objects:

Command-line functions and objects are available in the following categories:

- Discrete-time filter design, analysis, and implementation
- Analog filter design, analysis, and implementation
- Linear system transformations
- Windowing functions
- Spectral analysis and cepstral analysis
- Transforms
- Statistical signal processing
- Parametric modelling
- Linear prediction
- Multirate signal processing
- Waveform generation

Graphical User Interfaces

A suite of interactive graphical user interfaces are available for

- Filter design and analysis
- Window design and analysis

- Signal plotting and analysis, spectral analysis, and filtering

Supported Data Types

The Signal Processing Toolbox software supports only double-precision inputs. If input is single-precision floating-point or integer data in many cases error will occur. The Filter Design Toolbox product, in conjunction with the Fixed-Point Toolbox™ product, enables single-precision floating-point and fixed-point support for filtering and filter design.

B. The Filter Design Toolbox™

Filter Designer is a powerful graphical user interface (GUI) in the Signal Processing Toolbox™ for designing and analysing filters. Filter Designer enables the user to quickly design digital FIR or IIR filters by setting filter performance specifications, by importing filters from your MATLAB® workspace or by adding, moving, or deleting poles and zeros. Filter Designer also provides tools for analysing filters, such as magnitude and phase response plots and pole-zero plots.

The GUI has three main regions:

i. The Current Filter Information region
ii. The Filter Display region and
iii. The Design panel

The upper half of the GUI displays information on filter specifications and responses for the current filter. The Current Filter Information region, in the upper left, displays filter properties, namely the filter structure, order, number of sections used and whether the filter is stable or not. It also provides access to the Filter manager for working with multiple filters.

The Filter Display region, in the upper right, displays various filter responses, such as, magnitude response, group delay and filter coefficients. The lower half of the GUI is the interactive portion of Filter Designer. The Design Panel, in the lower half is where user can define filter specifications. It controls what is displayed in the other two upper regions. Other panels can be displayed in the lower half by using the sidebar buttons. The following functionality can be achieved using it.

- Magnitude response
- Phase response
- Magnitude and Phase responses
- Group delay response
- Phase delay response
- Impulse response
- Step response
- Pole-zero plot
- Filter Coefficients
- Filter Information

C. **Wavelet Toolbox™**

Signal and image can be analysed in Wavelet Toolbox™. The toolbox includes algorithms for continuous wavelet analysis, wavelet coherence, synchrosqueezing, and data-adaptive time-frequency analysis. The toolbox also includes apps and functions for decimated and nondecimated discrete wavelet analysis of signals and images, including wavelet packets and dual-tree transforms.

It can be explore how spectral features evolve over time, identify common time-varying patterns in two signals, and perform time-localized filtering using continuous wavelet analysis. Discrete wavelet analysis ca be used to analyse signals and images at different resolutions to detect change points, discontinuities, and other events not readily visible in raw data. Signal statistics on multiple scales can be compared and fractal analysis of data can be performed to reveal hidden patterns. With Wavelet Toolbox user can obtain a sparse representation of data, useful for denoising or compressing the data while preserving important features.

The Wavelet Toolbox™ GUI can be accessed by typing the command '*wevmenu*' in the MATLAB command line. The menu of Wavelet Toolbox™ has been shown in the figure bellow

Figure: 4.5. Wavelet Toolbox menu

***

[5] RESULTS AND DISCUSIONS

The raw ECG recordings has been taken from PhysioBank database. 10 preterm infant subjects and 10 normal sinus rhythm[41][98]. The sampling frequency of the preterm infant ECG data is 500 Hz whereas the sampling frequency of the normal sinus data is 128 Hz. According to the guideline by American Society of pacing 128Hz ECG is enough for HRV analysis [1]. So the sampling frequency of the selected data is sufficient

Powerline Interference Filtering using Notch Filter:

Typical ECG has Powerline Interference embedded in it. If power spectral analysis is done that can be seen clearly. The figure 5.2 is the power spectral plot of the ECG signal of figure 5.1. Which is showing two peaks at 60 Hz and 120 Hz. This is because of the PLI of 60 Hz power supply. A As 120Hz is the image frequency of 60 Hz a peak is present there too. To eliminate this a notch filter centred at 60 Hz has been designed in the MATLAB signal processing (SP tool) tool box. The transfer function has been shown in figure 5.3.

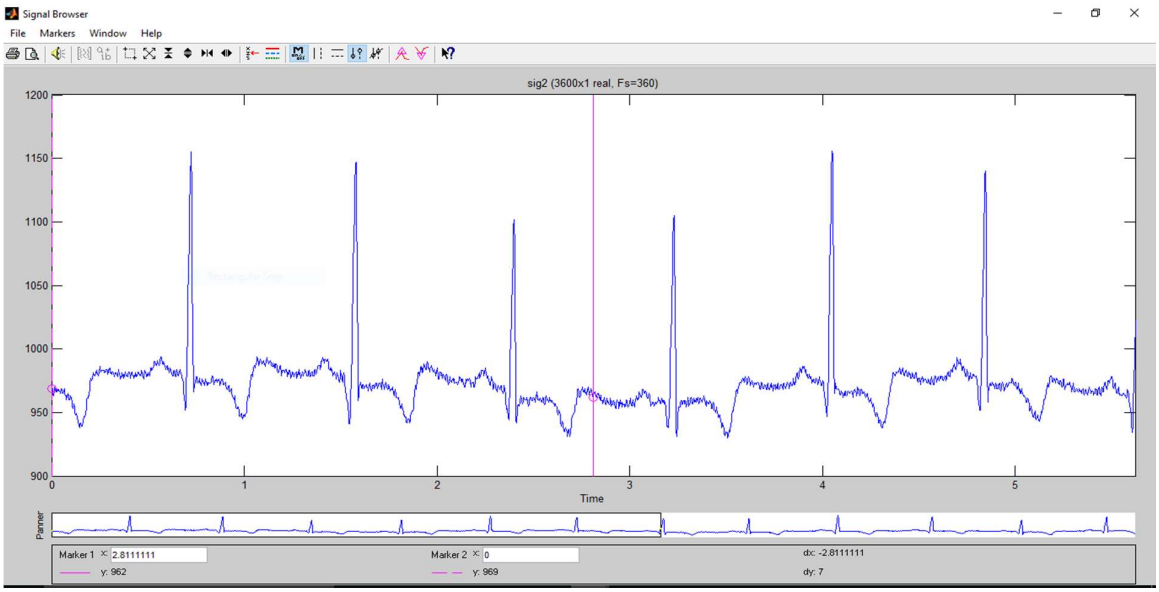

Figure: 5.1. Normal sinus ECG

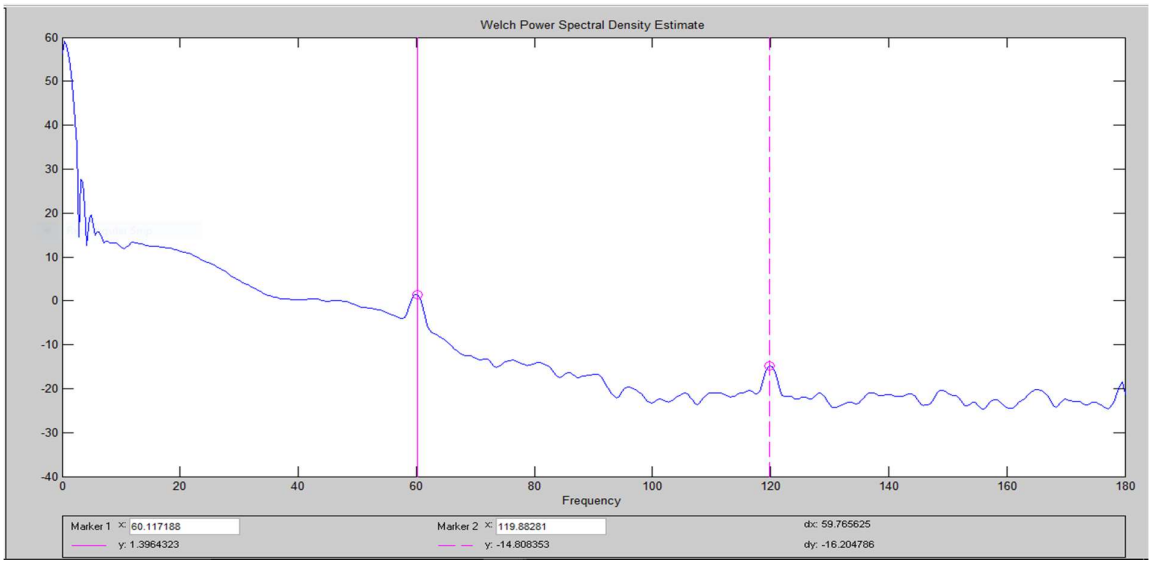

Figure: 5.2. Power spectral density of the ECG signal

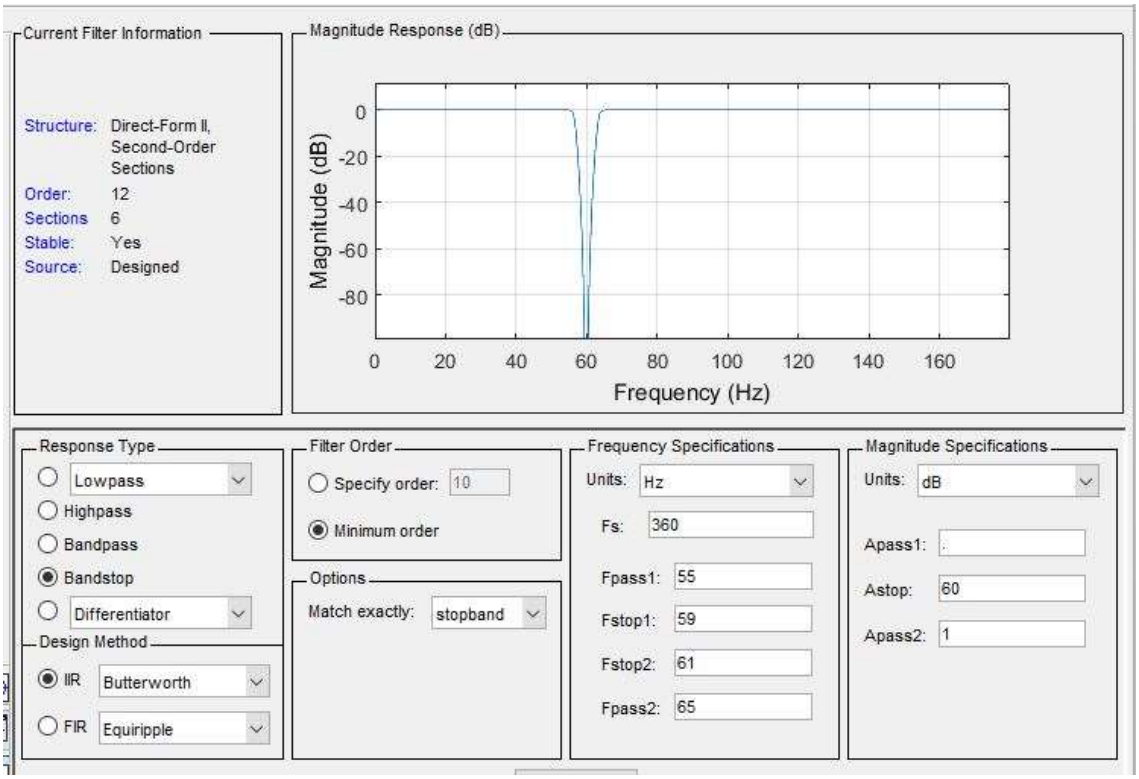

Figure: 5.3. 60 Hz Notch filter magnitude response

After implementing the 12 order 60 Hz Notch filter (Chebyshev type II) the spectrum of the signal is analysed. The spectrum is given in figure 5.5. The 60 Hz component is not there. But as ECG signal has 60 Hz component also by implementing notch filter we are not just eliminating the powerline component the ECG part of the 60 Hz has also been removed. This is unexpected while reducing noise. One approach can be based on FFT decomposition. We have to derive the power component at 60 Hz and its neighbourhood. Then using

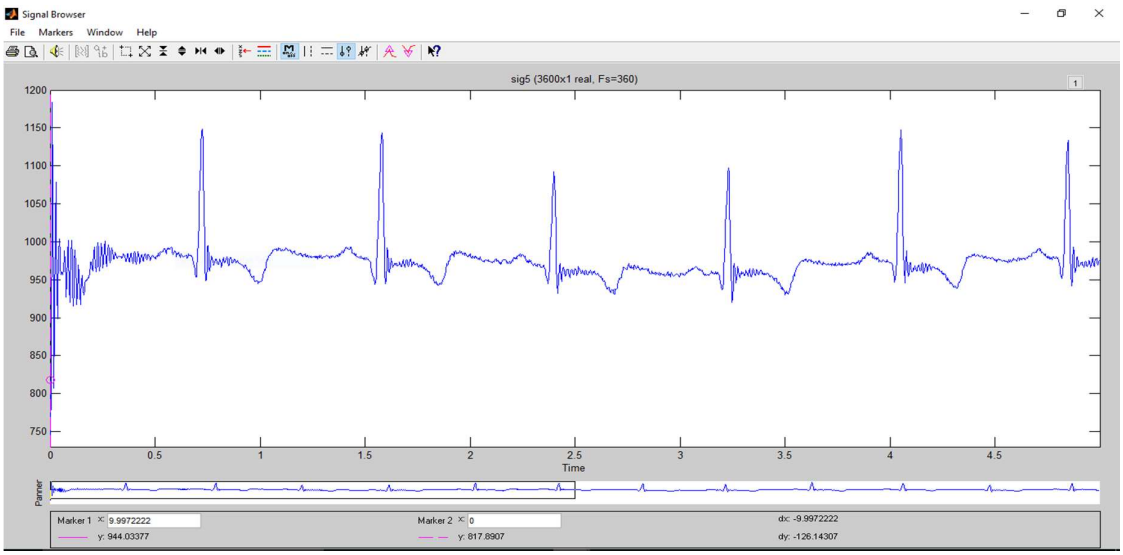

Figure: 5.4. 60 Hz PLI filtered ECG signal

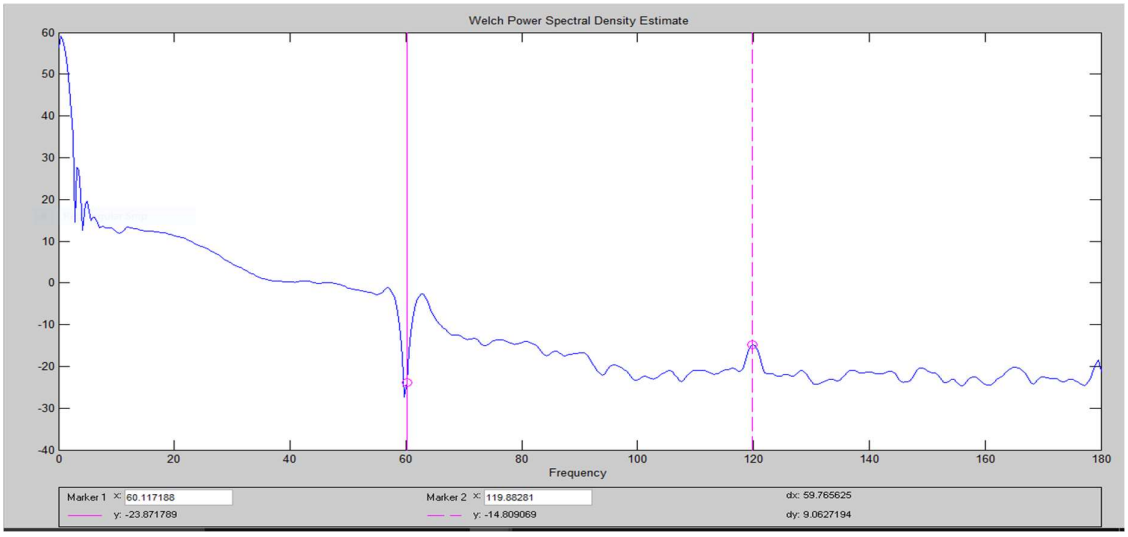

Figure: 5.5. Power spectral density of 60 Hz PLI eliminated ECG signal

R Peak Detection:

If the ECG signal is fully noise free with out baseline wander the peak detection algoithm based on peak threshold method can easily be implemented to detect the R peaks of a ECG signal. But the ECG signal available are not always noise free. It has base line wonders, movement artifacts, contact noise. Other than this different cardiopathic condition might itself can make a peak absence. So for a computer program it is ambiguous to detect those peaks. A normal synus rhythm ECG has been ploted allong with its detected R peak in figure . The signal has been taken from MIT-BIH database.

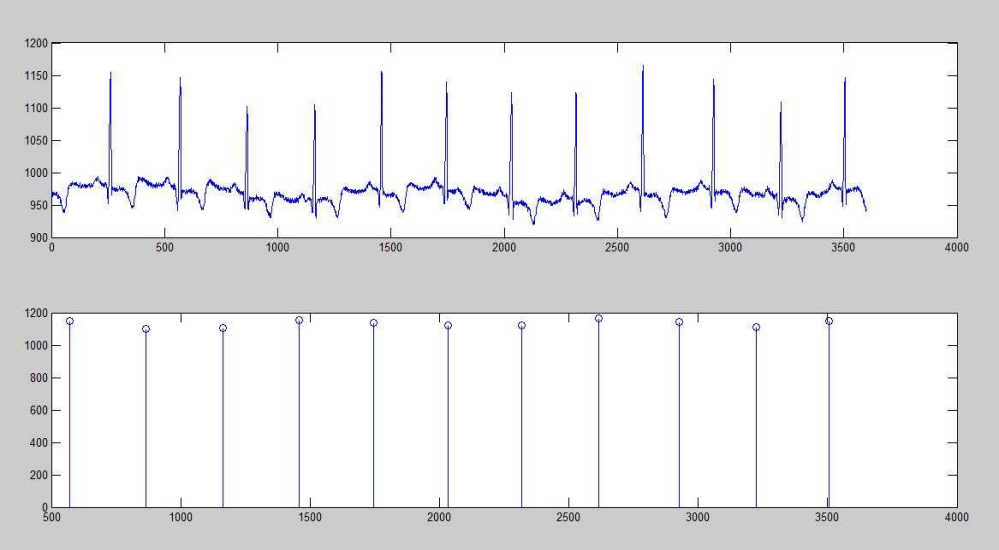

Figure: 5.6. Normal Sinus Rhythm ECG along with its detected R peak.

The first step toward HRV analysis is to detect the respective normal components of all the cardiac cycle throughout the entire ECG data. For convenience the R peak is generally chosen as the normal component as it has highest amplitude value so it has better detection possibility. Now the ECG signal we get is not ideal. It has base line wanders, muscle noise and other artefacts presents. Moreover there are multiple types of peaks present in a single

ECG waveform. Which makes detection of the normal components a challenging task. One such example is shown in the figure 5.7.

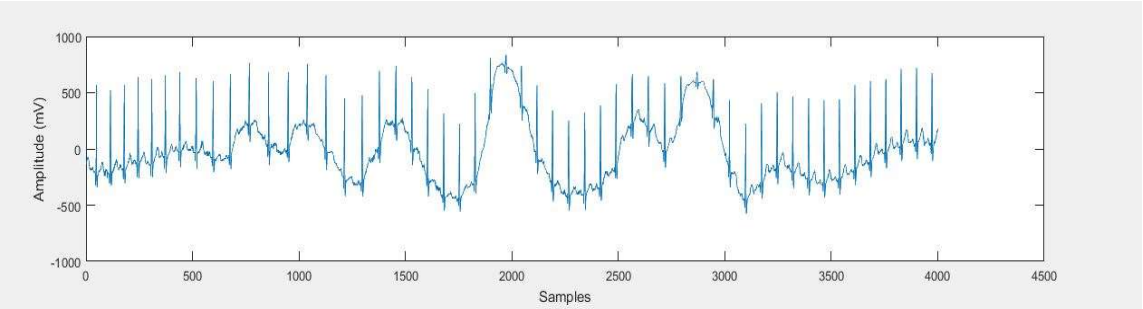

Figure: 5.7. ECG signal with baseline wonder.

Now to make a universal peak detector the situation become more complex to detect the correct peaks as there is widely varying ECG features in ECG waveform between different physiological conditions. So normal inbuilt peak detection algorithms based on constant thresholding are not sufficient.

To achieve this some pre-processing is done before passing it to the peak detector. Wavelet transformation is very useful in this job. Wavelet denoising technique is a very efficient tool to give rise the R peak and supress other features. This decreases the ambiguity of R peak detection for the detection by increasing the amplitude difference between the R peaks and other peaks i.e. P, T etc.

The signal has been denoised with Haar level 8 wavelet decomposition technique. A wavelet denoised signal of such data set has been shown in figure 5.9. It is visible that the P and T peaks have been reduced significantly leading to reduced ambiguity of R peak detection.

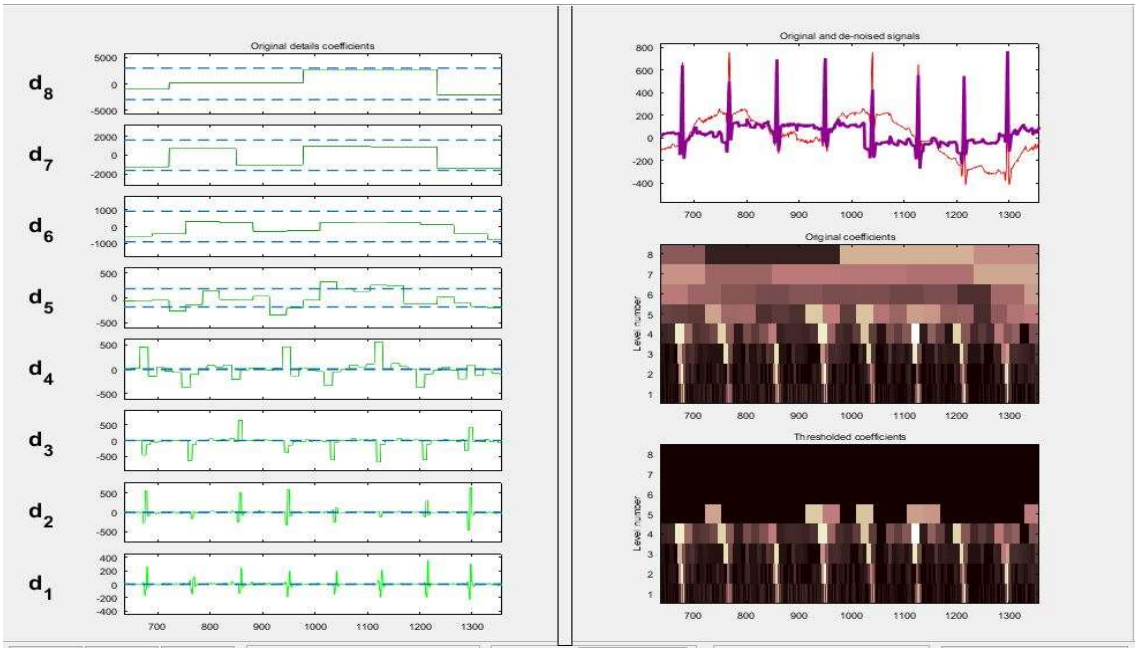

Figure: 5.8 Wavelet denoising of ECG signal

Figure: 5.9. The comparison between wavelet denoised version with the noisy ECG

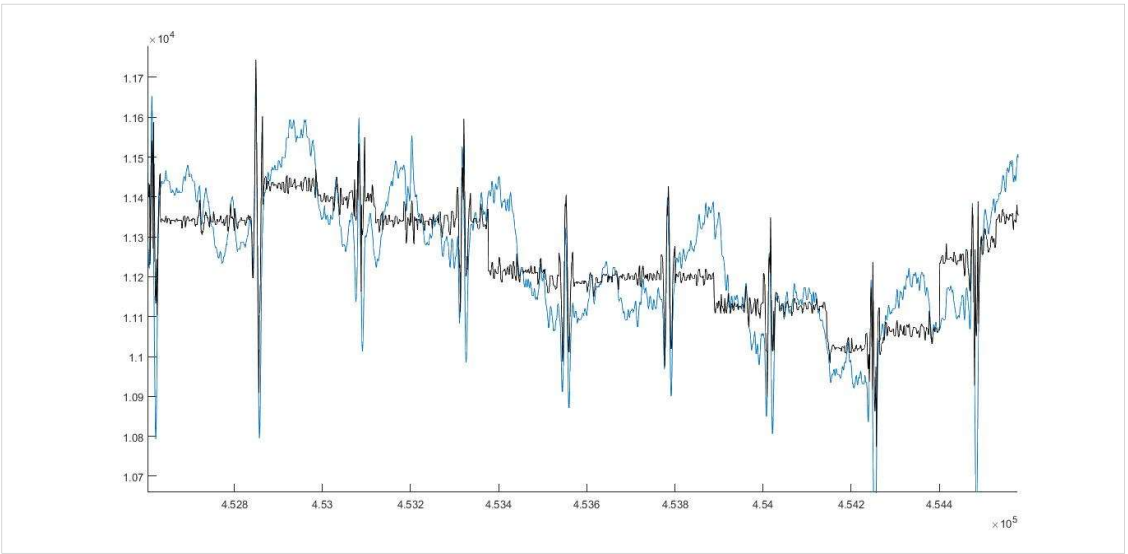

(Blue: noisy ECG; Black wavelet denoised version)

With the help of peak prominence and minimum peak distance threshold an ambiguous R peak has been correctly detected (figure 5.10).

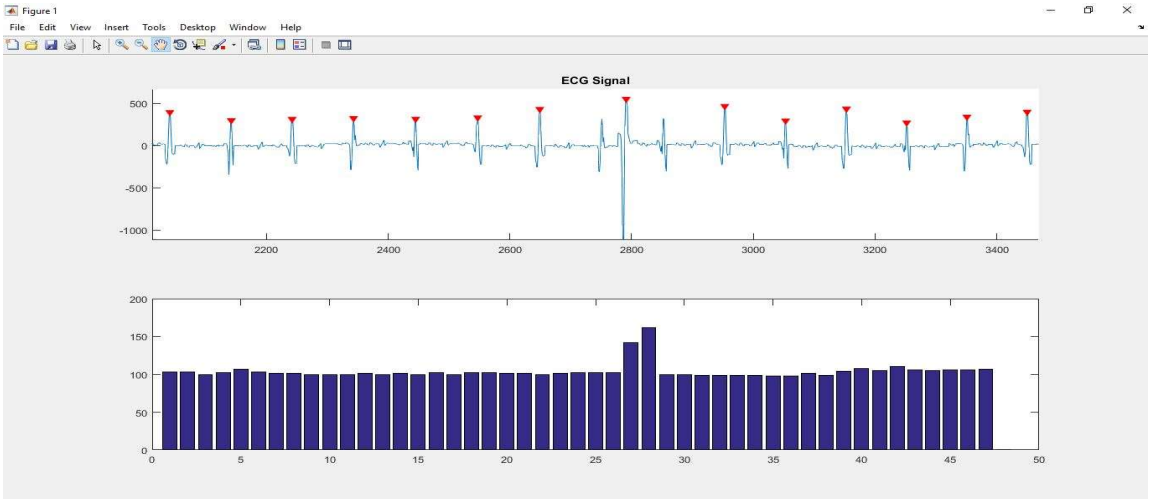

Figure: 5.10. Detection of R peak from ambiguous situation with the help of minimum peak distance thresholding

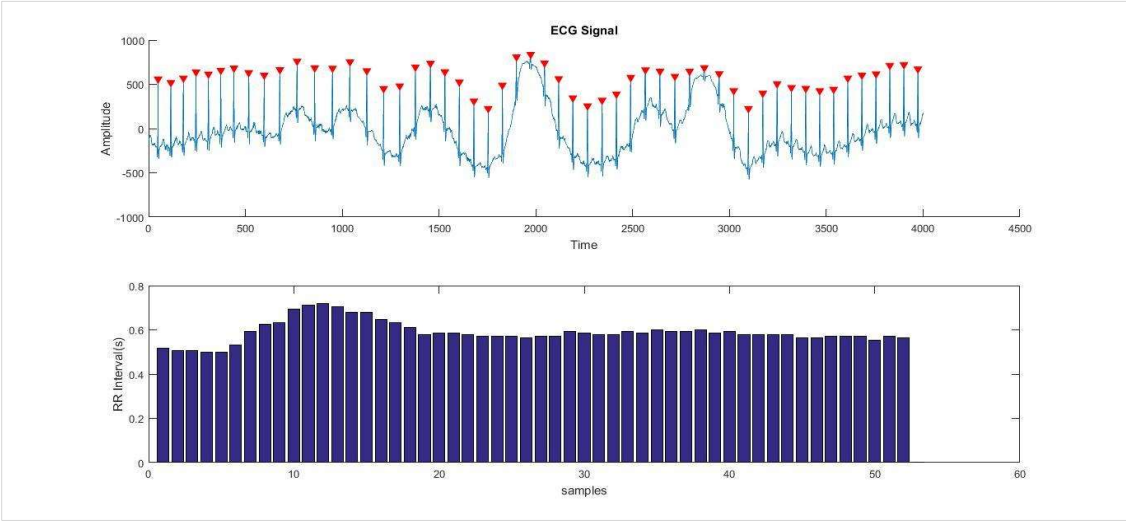

Figure: 5.11. Peak detection achieved in noisy ECG

Using the developed algorithm ECG of 10 Preterm Infant have been studied. The HRV parameter has been determined. Then compared with 10 Normal Sinus Rhythm ECG HRV parameters. The preterm infant ECG and the Normal Sinus ECG has been taken from MIT-BIH database. The Results has been given in the table bellow

Preterm RR Mean (s)	NSR RR Mean (s)	Preterm Standard Deviation(s)	NSR Standard Deviation	Preterm variance (s^2)	NSR Variance (s^2)	Preterm Heart Rate (Beats / s)	NSR Heart Rate (Beats / s)	Preterm LF/HF	NSR LF/HF
0.385218	0.700609	0.018789	0.101116	0.000353	0.010224	155.7	85.63983	0.1546	1.5600
0.506569	0.820988	0.025362	0.120630	0.000643	0.014552	117.9	73.08265	0.5859	1.4019
0.506547	0.863663	0.028371	0.197354	0.000805	0.038949	118.4	69.47158	0.6139	2.6840
0.381531	0.804766	0.014206	0.133408	0.000202	0.017798	104.8	74.55587	0.3455	2.2324
0.397890	0.585845	0.025011	0.071947	0.000626	0.005176	150.7	102.4161	0.1835	3.0727
0.449316	0.699586	0.016618	0.095919	0.000276	0.009200	133.4	85.76502	1.0467	1.9977
0.410908	0.607548	0.023058	0.091041	0.000532	0.008289	145.9	98.75768	0.8265	2.3355
0.452145	0.732770	0.024633	0.078748	0.000607	0.006201	132.6	81.88113	1.0216	1.0542
0.426246	0.883962	0.018451	0.075674	0.000340	0.005727	140.7	67.87624	0.9925	1.9377
0.385698	0.641930	0.037447	0.049798	0.001402	0.002480	155.5	93.46807	0.4933	1.9170

Table: 5.1. Comparison of NSR and Preterm Infant ECG

The mean of the 10 ECG data of two different group has been plotted in figure 5.12 and figure 5.16. It is clear that the mean of the Normal Sinus Rhythm RR intervals is significantly higher than the preterm infants. This indicates the heart rate of the preterm infant is significantly higher.

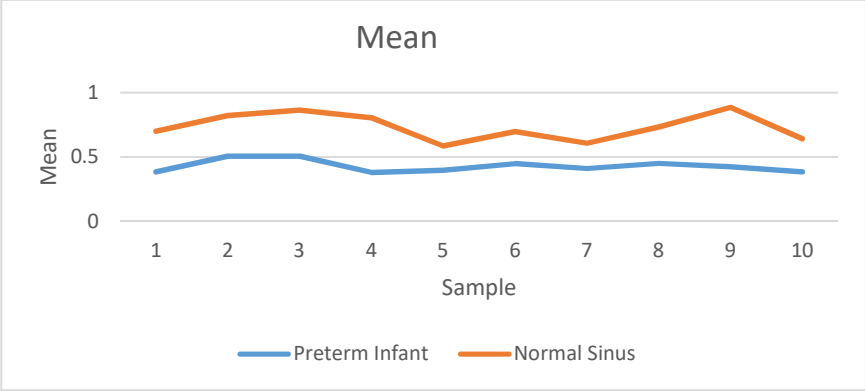

Figure: 5.12. Comparison between mean of Preterm infant ECG and Normal Sinus RR intervals

The standard deviation and variance of the 10 ECG data of two different group has been plotted in figure 5.13 and figure 5.14 respectively. It is visible that the dispersion of the

instantaneous heart rate of the Normal Sinus Rhythm RR interval is significantly lower than the Normal Sinus rhythm ones. This indicates the heart rate variability of the preterm infant is significantly lower compared to Normal Sinus rhythm.

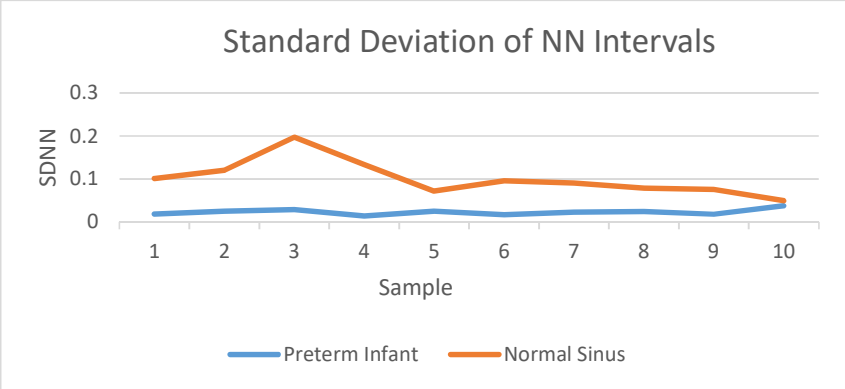

Figure: 5.13. Comparison between SDNN of Preterm infant ECG and Normal Sinus RR intervals

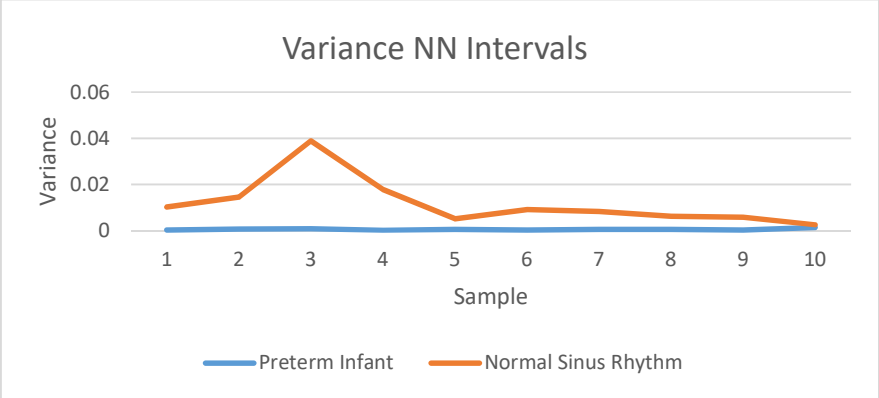

Figure: 5.14. Comparison between variance of NN interval Preterm infant ECG and Normal Sinus RR intervals

The LF/HF ratio of the 10 ECG data of two different group has been plotted in figure 5.15. Here also the LF/HF parameter in higher most of the cases. This might be the result of

undeveloped autonomic nervous system in preterm infant. The LF/HF parameter indicates the vagal balance of autonomic nervous system.

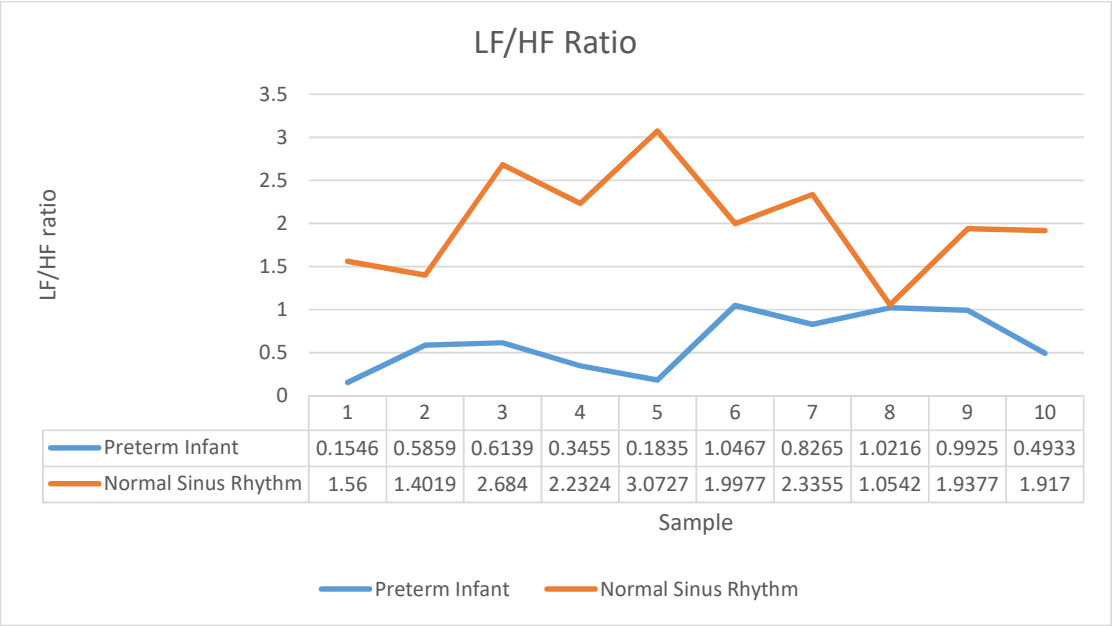

Figure: 5.15. Comparison between LF/HF power ratio of Preterm infant ECG and Normal Sinus Rhythm RR intervals

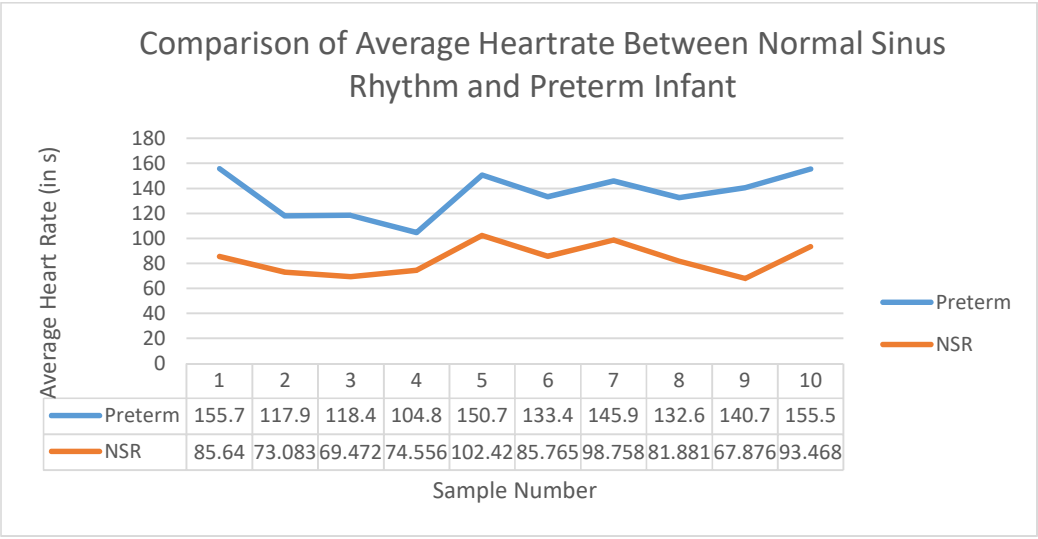

Figure: 5.16. Comparison between Heart Rate of Preterm infant ECG and Normal Sinus Rhythm RR intervals

The sample to sample variation in above estimated parameters show less deviation in case of Preterm infant subjects with relatively smooth trends than normal adult with abrupt changes. Further studies are required in this part to accurately suggest a methodology for robust and reliable analysis of preterm infant ECG.

.

***

[6] CONCLUSION

In this work it has been proposed an approach for robust estimation of the RR series and their HRV analysis technique from a noise & motion artefact corrupted ECG signal. The heart rate variability found to be significantly lower in case of preterm infant children studied than the Normal sinus ones. This indicate that the statistical and frequency domain HRV parameters can be used as a bio-marker under standard diagnostic protocol. This study opens the area of studying preterm infant ECG signals and identify the differences it has from normal sinus ECG. We have observed significant differences in the values of estimated parameters for normal and preterm infant ECG signals. Preterm infant ECG signal has wide differences in HRV trends from those of normal sinus rhythms of adults

***

[7] FUTURE PROSPECTS OF THE WORK

Comparative study might be carried out by employing different denoising methods using different wavelets. Machine learning algorithm can be employed to denoise, peak detection and feature extraction. HRV mainly caused by ANS regulation. So with good feature extraction technique research on human emotion relating to HRV might be carried out. Which will make the path for Human Computer Interfacing.

Diseased ECG signal can be studied using it. The bio marking capability of the HRV for disease condition can be checked. That might lead to a better efficient disease detection protocol. Which can be implemented in microprocessor based systems. This has the possibility of making IOT with biomedical sensors and our general purpose computer and smartphone.

***

[8] REFERENCES

[1] "Task force of the European society of cardiology and the North American society of pacing and electrophysiology. Heart rate variability – standards of measurement, physiological interpretation, and clinical" use. *Circulation*, 93(5):1043–1065, March 1996.

[2] Acharya UR, Joseph KP, Kannathal N, Lim CM, Suri JS. "Heart rate variability: A review," *Med Bio Eng Comput* 2006; 44:1031–1051.

[3] Clifford, G.D.; Azuaje F.; McSharry, "P.E.: Advanced Methods and Tools for ECG Data Analysis", Artech house, ISBN-13: 978-1-58053-966-1 (2006)

[4] Wung, N.C.; Hung, J.W.; Lee, "L.S.: Data driven temporal filters based on multi-eigen vector for robust feature in speech recognition", IEEE International Conference on Acoustics, Speech, and Signal Processing, pp. I400–I403 (2003)

[5] Chazal, P.D.; Reilly, R.B.: A comparison of the ECG classification performance of different feature sets", IEEE

[6] Elgendi M, Eskofier B, Dokos S, Abbott D. "Revisiting QRS detection methodologies for portable, wearable, battery-operated, and wireless ECG systems." PLoS One. 2014; 9(1):e84018. PM id: 24409290, http://dx.doi.org/10.1371/journal.pone.0084018. Comput. Cardiol 27, 327–330 (2000)

[7] Sörnmo L, Laguna P. "Bioelectrical signal processing in cardiac a neurological applications." Elsevier Academic Press; 2005

[8] Rangayyan RM. "Biomedical signal analysis: a case-study approach." IEEE Press Ser Biomed Eng 2002.

[9] Webster JG, editor. "Medical instrumentation: application and design." 4th ed, Hoboken: John Wiley and Sons; 2010

[10] Lobodzinski SS, Laks MM, "New devices for very long-term ECG monitoring", Cardiol J. 2012; 19(2):210-4, PM id: 22461060, http://dx.doi.org/10.5603/CJ.2012.0039.

[11] Oppenheim AV, Schafer RW. Discrete-time signal processing. 3rd ed. Upper Saddle River: Prentice-Hall; 2010.

[12] Jha P, Patra P, Naik J, Dutta A, Acharya A, Rajalakshmi P, Singh SGA. "2µW biomedical frontend with ΣΔ ADC for self-powered U-healthcare devices in 0.18µm CMOS technology." In: Proceedings of the IEEE 13th New Circuits and Systems Conference; 2015 Jun 7-10;

Grenoble, France. United States: IEEE; 2015. p. 1-4. http://dx.doi.org/10.1109/NEWCAS.2015.7182054.

[13] Komorowski D, Andrzej M, Stanislaw P. Hybrid system of ECG signal acquisition and QRS complexes detection for special medical devices synchronization. JMIT. 2013; 22:227-34.

[14] Romero RA, Silva GM, and Sousa FR. "A duty-cycle controlled variable-gain instrumentation amplifier applied for two-electrode ECG measurement." in Proceedings of the IEEE Instrumentation and Measurement Technology Conference; 2012 May 13-16; Graz, Austria. United States: IEEE; 2012. p. 1270-74.

[15] Yamakawa T, Matsumoto G, Aoki T. "A low-cost long-life R-R interval telemeter with automatic gain control for various ECG amplitudes," Journal of Advanced Research in Physics, 2012 [cited 2017 Jul 24]; 3(1):011205.

[16] J.A. Van Alste, T.S. Schilder, "Removal of base-line wander and power line interference from the ECG by an efficient FIR filter with a reduced number of taps", in: Proceedings of the 2nd International Conference on vol. 32, 1985, pp.1052–1060.

[17] T. Slonim, M.A. Slonim, E. Ovsyscher, "The use of simple FIR filters for filtering of ECG signals and a new method for post-filter signal reconstruction," in: Proceedings of Computers in Cardiology Conference, London, 1993, pp. 871–873.

[18] M.S. Chavan, R.A. Agarwala, M.D. Uplane, "Suppression of baseline wander and power line interference in ECG using digital IIR filter", Int. J. Circuit Syst. Signal Process. 2 (2) (2008) 132–142.

[19] S. Cuomo, G. De Pietro, R. Farina, A. Galletti, G. Sannino, "A O(n) novel numerical scheme for ECG signal denoising", Proc. Comput. Sci. 51 (2015) 775–784.

[20] V. Alfonso, W. Thomkins, T. Nguyen, S. Trautmann, S. Luo, "Filter bank-based processing of the stress ECG", in: Proceedings of the 17th IEEE Engineering in Medicine and Biology Society Conference vol. 2, 1995, pp. 887–888.

[21] S. Hargittai, "Savitzky-Golay least-squares polynomial filters in ECG signal processing", in: Proceedings of the Computers in Cardiology, Lyon, 2005, pp.763–766.

[22] K.M. Chang, S.H. Liu, "Gaussian noise filtering from ECG by wiener filter and ensemble empirical mode decomposition", J. Signal Proc. Syst. 64 (2011)249–264.

[23] N.V. Thakor, Y.-S. Zhu, "Applications of adaptive filtering to ECG analysis: noise cancellation and arrhythmia detection", IEEE Trans. Biomed. Eng. 38 (8) (1991Aug) 785–794.

[24] J. Jenitta, A. Rajeswari Dr., “Denoising of ECG signal based on improved adaptive filter with EMD and EEMD”, in: Conference on Information and Communication Technology, 2013, pp. 957–962.

[25] G.M.S. Sajjad, H. Rahman, A.K. Dey, A.M. Biswas, Z. Islam, A.K.M.J. Hoque, “Performance comparison of modified LMS and RLS algorithms in denoising of ECG signals”, Int. J. Eng. Technol. 2 (3) (2012) 466–468.

[26] C. Chandrakar, M.K. Kowar, Denoising ECG signals using adaptive filter algorithm, Int. J. Soft Comput. Eng. 2 (1) (2012) 120–123.

[27] M. Rahman, R. Shaik, D. Reddy, “Adaptive noise removal in the ECG using the Block LMS algorithm”, in: Proceedings of the 2nd International Conference onAdaptive Science and Technology (ICAST), 2009, pp. 380–383.

[28] Y. Weiting, Z. Runjing, “An improved self-adaptive filter based on LMS algorithm for filtering 50 Hz interference in ECG signals”, in: Proceedings of the 8th International Conference on Electronic Measurement and Instruments ICEMI’07, 2007,pp. 3-874–3-878.

[29] M. Rahman, R. Shaik, D. Reddy, “Noise cancellation in ECG signals using normalized sign-sign LMS algorithm”, in: Proceedings of the IEEE International Symposium on Signal Processing and Information Technology, (ISSPIT), 2009,pp. 288–292.

[30] S. Olmos, L. Sörnmo, P. Laguna, Block adaptive filters with deterministic ref-erence inputs for event-related signals: BLMS and BRLS, IEEE Trans. SignalProcess. 50 (5) (2002) 1102–1112.

[31] S.A. Rehman, R.R. Kumar, Performance comparison of adaptive filter algorithmsfor ECG signal enhancement”, Int. J. Adv. Res. Comput. Commun. Eng. 1 (2)(2012).

[32] C.B. Mbachu, et al., Processing ECG signal with Kaiser window-based FIR digital filters, Int. J. Eng. Sci. Technol. 3 (8) (2011) 6675–6783, August

[33] SeemaVerma, Reduction of noise from ECG signal using FIR low pass filter with various window techniques Eng. Sci. Technol. J.1 (5) (2013) 117–122, July

[34] Rupali Madhukar Narsale, Dhanashri Gawali, Amit Kulkarni, FPGA based design & implementation of low power FIR filter for ECG Signal Process.” Int J. Sci. Eng.Technol. Res. 3 (6) (2014) 1673, June

[35] Manoj Sharma, Hemant Dalal, Designing and implementation of digital filter for power line interference Suppression Int. J. Sci. Eng. Technol. Res. 3 (6) (2014) 1831–1836, June

[36] McManus, C.D.; Teppner, U.; Neubert, D. and Lobodzinski S.M. 1985“Estimation and Removal of Baseline Drift in the Electrocardiogram”, Computers and Biomedical Research, 18, issue 1, February, pp. 1-9

[37] Sornmo, L. 1993, “Time-Varying Digital Filtering of ECG Baseline Wander,”Medical and Biological Engineering and Computing, 31, Number 5pp. 503-508

[38] Allen, J.; Anderson, J. Mc C.; Dempsey, G.J.; Adgey A.A.J.; 1994, “Efficient Baseline Wander Removal for Feature “Efficient Baseline Wander Removal for Feature,” IEEE Proceedings of Engineering in Medicine and Biology Society 2, pp 1316– 1317

[39] Choy T.T., Leung P.M., “Real Time Microprocessor-Based50 Hz Notch Filter for ECG,”J. Biomed Eng.1988 May; 10 (3): 285-8

[40] Markovsky, Ivan A.; Anton, Van H. and Sabine, 2008“Application of Filtering Methods for Removal Of Resuscitation Artefacts from Human ECG Signals.” IEEE Conference of Engineering in Medicine and Biology Societypp 13-16

[41] Goldberger AL, Amaral LAN, Glass L, Hausdorff JM, Ivanov PCh, Mark RG, Mietus JE, Moody GB, Peng C-K, Stanley HE. PhysioBank, PhysioToolkit, and PhysioNet: Components of a New Research Resource for Complex Physiologic Signals. Circulation 101(23), pp. 215-220, 2000.

[42] https://www.ncbi.nlm.nih.gov/books/NBK11075/

[43] http://www.freedive-earth.com/file/ans-and-heart-rate

[44] https://en.wikipedia.org/wiki/Autonomic_nervous_system

[45] Lebedeva S.V., Lebedev V.V., “Digital Filter for Circuit Noise Suppression in the Electrocardiograph.” Med Tekh.1995Sep-Oct; (5):23-5

[46] Daqrouq, K. 2005, “ECG Baseline Wandering Reduction Using Discrete Wavelet Transform.” Asian Journal of Information Technology4.issue 11, pp 989-995

[47] Zhang, D. 2005, “Wavelet Approach for ECG Baseline Wander Correction and Noise Reduction”, Proceedings of the IEEE on Engineering in Medicine and Biology 27thAnnual Conference, pp 1212-1215

[48] Sayadi, O.; Mohammad B.S. 2007, “ECG Baseline Correction with Adaptive Bionic Wavelet Transform”,IEEE

[49] A.K. Barros, A. Mansour, N. Ohnishi, Removing artifacts from electrocardio-graphic signals using independent components analysis, Neurocomputing 22(1-3) (1998) 173–186.

[50] J.S. Paul, M.R.S. Reddy, J. Kumar, Data processing of stress ECG using discretecosine transform, Comput. Biol. Med. 28 (6) (1998) 639–658.

[51] W. Zhaohua, H. Norden E, Ensemble empirical mode decomposition: a noiseassisted data analysis method, in: Advances in Adaptive Data Analysis, 2009,pp. 1–41.

[52] N. Pan, V. Mang I, M. Peng Un Pun Sio Hang, Accurate removal of baselinewander in ECG using empirical mode decomposition, in: Proceedings of theJoint Meeting of the 6th

International Symposium on Noninvasive FunctionalSource Imaging of the Brain and Heart and the International Conference onFunctional Biomedical Imaging, 2007, pp. 177–180.

[53] C. Kang-Ming, Arrhythmia ECG noise reduction by ensemble empirical modedecomposition, Sensors 10 (6) (2010) 6063–6080.

[54] G. Singh, G. Kaur, V. Kumar, ECG denoising using adaptive selection of IMFsthrough EMD and EEMD, in: Proceedings of the International Conference onData Science & Engineering (ICDSE), 2014, pp. 228–231.

[55] V. Prasad, T.S. Latha, M. Suresh, Denoising of biological signals using wavelets,Int. J. Curr. Eng. Technol. 3 (3) (2013) 863–866.

[56] R. Cohen, Signal Denoising Using Wavelets, 2012, Project Report (http://tx.technion.ac.il/rc).

[57] K. Daqrouq, ECG baseline wander reduction using discrete wavelet transform,Asian J. Inf. Technol. 4 (11) (2005) 989–995.

[58] B. Arvinti, M. Costache, D. Toader, M. Oltean, A. Isar, ECG statistical denoising inthe wavelet domain, in: Proceedings of the 9th IEEE International Symposiumon Electronics and Telecommunications, 2010, pp. 307–310.

[59] K. Daqrouq, A.-R. Al-Qawasmi, ECG enhancement using wavelet transform,WSEAS Trans. Biol. Biomed. 7 (2) (2010) 62–72.

[60] G. Georgieva-Tsaneva, K. Tcheshmedjiev, Denoising of electrocardiogram datawith methods of wavelet transform, in: Proceedings of the International Con-ference on Computer Systems and Technologies, 2013, pp. 9–16.

[61] M.F.M. Kania, Wavelet denoising for multi-lead high resolution ECG signals,Meas. Sci. Rev. 7 (2) (2007).

[62] P.S. Gokhale, ECG signal de-noising using discrete wavelet transform forremoval of 50Hz PLI noise, Int. J. Emerg. Technol. Adv. Eng. 2 (5) (2012)81–85.

[63] O. Sayadi, M.B. Shamsollahi, Multiadaptive bionic wavelet transform: applica-tion to ECG denoising and baseline wandering reduction, EURASIP J. Adv. SignalProcess. 2007 (2007), http://dx.doi.org/10.1155/2007/41274, Article ID 41274,11 p.

[64] M. Alfaouri, K. Daqrouq, ECG signal denoising by wavelet transform threshold-ing, Am. J. Appl. Sci. 5 (3) (2008) 276–281.

[65] G. Georgieva-Tsaneva, K. Tcheshmedjiev, Denoising of electrocardiogram datawith methods of wavelet transform, in: Proceedings International Conferenceon Computer Systems and Technologies Compsystech'13, 2013, pp. 9–16.

[66] H.A. Kestler, M. Haschka, W. Kratz, et al., De-noising of high-resolution ECG signals by combining the discrete wavelet transform with the Wiener filtering: Proceedings Computers in Cardiology, September, Cleveland, OH, 1998, pp.233–236.
[67] Q. Zhang, A. Benveniste, Wavelet Networks, IEEE Trans. Neural Netw. 3 (6) (1992November) 889–898.
[68] S. Poungponsri, X. Yu, Electrocardigram (ECG) signal modeling and noise reduc-tion using wavelet neural networks, in: Proceedings of the IEEE International Conference on Aut and Logis, 2009, pp. 394–398.
[69] S. Poungponsri, X. Yu, An adaptive filtering approach for electrocardiogram(ECG) signal noise reduction using neural networks, Neuro computing 117 (2013)206–213.

[70] Brennan M, Palaniswami M, Kamen, P. "Do existing measures of poincaré plot geometry reflects nonlinear features of heart rate variability". *IEEE Transaction on Biomedical Engineering* 2001; 48:1342-1347.
[71] Eckberg DL. "Sympathovagal balance", *Circulation* 1997; 96:3224-3232.
[72]Goldberger AL. "Non-linear dynamics for clinicians: chaos theory, fractals, and complexity at the bedside", *Lancet* 1996; 347:1312-1314.
[73] Kaufmann T, Sütterlin S, Schulz SM, Vögele C. ARTiiFACT: A tool for heart rate artifact processing and heart rate variability analysis. *Behav Res* 2011; 43:1161-70.
[74] Kleiger RE. "Decreased heart rate variability and its association with increased mortality after acute myocardial infarction", *American Journal of Cardiology*1987; 59:256–262.
[75]. aHRV. HRV analysis software, http://www.nevrokard.eu/maini/hrv.html
[76]. Akselrod S, Gordan D, Ubel FA, Shannon DC, Barger AC, Cohen RC. Power spectrum analysis of heart rate fluctuation: A quantitative probe of beatto- beat cardiovascular control. *Science* 1981; 213:220-222.
[77]. Berntson GG, Bigger JT, Eckberg DL, Grossman P, Kaufmann PG, Malik M, Nagaraja HN, Porges SW, Saul JP, Stone PH, Vander Molen MW. Heart rate variability: origins, methods, and interpretive caveats. *Psychophysiology* 1997; 34:623-648.
[78]. Bigger JT, Albrecht P, Steinman RC, Rolnitzky LM, Fleiss JL, Cohen RJ. Comparison of time and frequency domain-based measures of cardiac parasympathetic activity in holter recordings after myocardial infarction. *American Journal of Cardiology* 1989; 64:536-538.
[79]. Brennan M, Palaniswami M, Kamen, P. Do existing measures of poincaré plot geometry reflects nonlinear features of heart rate variability. *IEEE Transaction on Biomedical Engineering* 2001; 48:1342-1347.

[80]. Eckberg DL. Sympathovagal balance. *Circulation* 1997; 96:3224-3232.

[81]. Goldberger AL. Non-linear dynamics for clinicians: chaos theory, fractals, and complexity at the bedside. *Lancet* 1996; 347:1312-1314.

[82] G.G. Berntson, J.T. Bigger Jr., D.L. Eckberg, P. Grossman, P.G. Kaufmann, M. Malik, H.N. Nagaraja, S.W. Porges, J.P. Saul, P.H. Stone, and M.W. Van Der Molen. Heart rate variability: Origins, methods, and interpretive caveats. *Psychophysiol*, 34:623–648, 1997.

[83] S.L. Marple. *Digital Spectral Analysis*. Prentice-Hall International, 1987.

[84] P. Tikkanen. *Characterization and application of analysis methods for ECG and time interval variability data*. PhD thesis, University of Oulu, Department of Physical Sciences, Division of Biophysics, 1999.

[85] M. Brennan, M. Palaniswami, and P. Kamen. Do existing measures pf Poincar´e plot geometry reflect nonlinear features of heart rate variability, *IEEE Trans Biomed Eng*, 48(11):1342–1347, November 2001.

[86] M.P. Tarvainen, P.O. Ranta-aho, and P.A. Karjalainen. An advanced detrending method with application to HRV analysis. *IEEE Trans Biomed Eng*, 49(2):172–175, February 2001.

[87] Antti Ruha, Sami Sallinen, and Seppo Nissil¨a. A real-time microprocessor QRS detector system with a 1-ms timing accuracy for the measurement of ambulatory HRV. *IEEE Trans Biomed Eng*, 44(3):159–167, March 1997.

[88] M. G. Poddar, V. Kumar and Y. P. Sharma, "Linear-nonlinear heart rate variability analysis and SVM based classification of normal and hypertensive subjects," in *J. of Electrocardioly*, vol. 46, no. 4, pp. e25, 2013.

[89] N. Natarajan, A. K. Balakrishnan and K. Ukkirapandian, "A study on analysis of Heart Rate Variability in hypertensive individuals," in *Int. J. of Biomedical and Advance Research*, vol. 5, no.2, pp. 109-111, 2014.

[90] M. Urooj, K. K. Pillai, M. Tandon, S. P. Venkateshan and N. Saha, "Reference ranges for time domain parameters of heart rate variability in indian population and validation in hypertensive subjects and smokers," Int J Pharm Pharm Sci.,vol. 3, pp. 36-39, 2011.

[91] Karthikeyan P, Murugappa M, Yaacob S. Detection of Human Stress
Using Short-term ECG and HRV analysis. 2013; 13: 38-67

[92] Ahmad Rauf Subhani, Likun Xia, Aamir Saeed Malik. Evaluation of mental stress using physiological signals. National Postgraduate Conference (NPC) 2011:pp. 1-4.

[94] L. Vanitha Hybrid SVM classification technique to detect mental stress in human beings using ECG signals. 2013 International Conference on Advanced Computing and Communication Systems, Coimbatore, 2013: pp. 1-6.

[95] D. S. Quintana, A. J. Guastella, T. Outhred, I. B. Hickie, and A. H. Kemp, “Heart rate variability is associated with emotion recognition: Direct evidence for a relationship between the autonomic nervous system and social cognition,” International Journal of Psychophysiology, vol. 86, no. 2, pp. 168 – 172, 2012.

[96] A. Gaurav, M. Maheedhar, V. N. Tiwari, and R. Narayanan, “Cuff-less ppg based continuous blood pressure monitoring - a smartphone based approach,” in 2016 38th Annual International Conference of the IEEE Engineering in Medicine and Biology Society (EMBC), Aug 2016, pp. 607–610.

[97] K. Choi, J. Kim, O. S. Kwon, M. J. Kim, Y. H. Ryu, J Park, “ Is heart rate variability (HRV) an adequate tool for evaluating human emotions?- A focus on the use of the International Affective Picture System(IAPS)”, Psychiatry Research 251, pp. 192-196, 2017, Elsevier Ireland ltd.

[98] Goldberger AL, Amaral LAN, Glass L, Hausdorff JM, Ivanov PCh, Mark RG, Mietus JE, Moody GB, Peng C-K, Stanley HE. PhysioBank, PhysioToolkit, and PhysioNet: Components of a New Research Resource for Complex Physiologic Signals. Circulation 101(23), pp. 215-220, 2000.

***